# Strengthened MILP Formulation for Combined-Cycle Units

Lei Fan, *Member, IEEE;* Kai Pan, *Student Member, IEEE;* Yongpei Guan, *Senior Member, IEEE;* Yonghong Chen; Xing Wang, *Senior Member, IEEE*

***Abstract*—Due to the increased utilization of gas-fired combined-cycle units for power generation in the U.S., accurate and computationally efficient models are more and more needed. The recently proposed edge-based formulation for combined-cycle units helps accurately describe the operations of combined-cycle units including capturing the transition processes and physical constraints for each turbine. In this paper, we derive tighter constraints and several families of strong valid inequalities to strengthen the edge-based model, by exploring the physical characteristics of combined-cycle units and utilizing the edge-based modeling framework. Meanwhile, we provide the validity and facet-defining proofs for certain inequalities. Finally, the computational experiment results indicate that our derived formulation significantly reduces the computational time, as the improved linear programming relaxation of our proposed formulation reduces the root-node gap significantly, which verifies the effectiveness of proposed constraints and strong valid inequalities.**

***Index Terms*—Combined-Cycle Units, Unit Commitment, Strong Valid Inequalities, Strong MILP Formulation.**

## I. Nomenclature

### A. Sets

| | |
|---|---|
| $\mathcal{A}$ | Arcs in the state transition graph. |
| $\mathcal{A}_k^{\text{all}}$ | Arcs linked to configuration $k$ in the state transition graph. |
| $\mathcal{A}_k^{\text{in}}$ | Incoming arcs of configuration $k$ in the state transition graph. |
| $\mathcal{A}_k^{\text{out}}$ | Outgoing arcs of configuration $k$ in the state transition graph. |
| $\mathcal{A}_k^{\text{sl}}$ | Self-loop arcs of configuration $k$ in the state transition graph. |
| $\mathcal{A}_i^{\text{sd}}$ | Arcs indicating turbine $i$ shuts down. |
| $\mathcal{A}_i^{\text{su}}$ | Arcs indicating turbine $i$ starts up. |
| $\mathcal{U}^{\text{CT}}$ | Combustion turbines (CTs) in a combined-cycle unit. |
| $\mathcal{U}^{\text{ST}}$ | Steam turbines (STs) in a combined-cycle unit. |
| $\mathcal{C}$ | Configurations in the state transition graph. |
| $\mathcal{C}_i^{\text{off}}$ | Configurations indicating turbine $i$ is offline. |
| $\mathcal{C}_i^{\text{on}}$ | Configurations indicating turbine $i$ is online. |
| $\mathcal{T}$ | Scheduling time periods. |

### B. Parameters

| | |
|---|---|
| $P_{\text{QS}}$ | Quick start capacity of a combined-cycle unit. |
| $\underline{P}_k$ | Minimal power output of configuration $k$ of a combined-cycle unit. |
| $\bar{P}_k$ | Maximal power output of configuration $k$ of a combined-cycle unit. |
| $\bar{P}^c$ | Total capacity of a combined-cycle unit. |
| $\text{RD}_a$ | Ramping down limit of arc $a$ in the transition graph. |
| $\text{RU}_a$ | Ramping up limit of arc $a$ in the transition graph. |
| $R_k^{\text{MS}}$ | Sustained ramping limit of configuration $k$ (MW/min). |
| $\text{SUC}_{\text{hot}}^i$ | Hot start-up cost of turbine $i$. |
| $\text{SUC}_{\text{warm}}^i$ | Warm start-up cost of turbine $i$. |
| $\text{SUC}_{\text{cold}}^i$ | Cold start-up cost of turbine $i$. |
| $\text{SDC}_i$ | Shut-down cost of turbine $i$. |
| $T_{\text{cold}}^i$ | Cold start time of turbine $i$. |
| $T_{\text{warm}}^i$ | Warm start time of turbine $i$. |
| $T_{\text{mu}}^i$ | Minimum online time for turbine $i$. |
| $T_{\text{md}}^i$ | Minimum offline time for turbine $i$. |

### C. Binary Decision Variables

| | |
|---|---|
| $z_t^a$ | Indicating the status of arc $a$ at time period $t$. |

### D. Continuous Decision Variables

| | |
|---|---|
| $oc$ | Operating cost of a combined-cycle unit. |
| $or_t$ | Operating reserve amount of a combined-cycle unit at time period $t$. |
| $p_t^k$ | Generation amount of configuration $k$ at time period $t$. |
| $p_t$ | Generation amount of a combined-cycle unit at time period $t$. |
| $pc_t$ | Generation cost of a combined-cycle unit at time period $t$. |
| $pc_t^k$ | Generation cost of a combined-cycle unit on configuration $k$ at time period $t$. |
| $sc_t$ | Status change cost (transition cost) of a combined-cycle unit at time period $t$. |
| $su_t^i$ | Start-up cost of turbine $i$ at time period $t$. |
| $sd_t^i$ | Shut-down cost of turbine $i$ at time period $t$. |
| $sr_t$ | Spinning reserve amount of a combined-cycle unit at time period $t$. |

## II. Introduction

Several factors such as fuel prices, environmental regulations, flexibility, and energy policies increase U.S. ISOs dependence on natural gas generation. For instance, MISO includes natural gas combined-cycle units in its future gener-

Lei Fan is with GE energy consulting, Schenectady, NY.

Kai Pan (co-first author) and Yongpei Guan are with the Department of Industrial and Systems Engineering, University of Florida, Gainesville, FL 32611. E-mail: guan@ise.ufl.edu.

Yonghong Chen is with Midcontinent Independent System Operator, Inc (MISO), Carmel, IN.

Xing Wang is with Centrica plc, Redmond, WA.

ation capacity expansions [1]. As the share of combined-cycle units in ISOs' generation portfolio increases, U.S. ISOs start to improve the model of combined-cycle units in their unit commitment models [2].

U.S. ISOs face two challenges when incorporating the combined-cycle unit models into traditional thermal unit commitment problems: (1) deriving an accurate model and (2) computational efficiency. The combined-cycle unit model is expected to accurately describe the operations of the combined-cycle unit. However, a more accurate model is usually more complicated, which leads to a heavy computational burden. Accordingly, it is challenging to keep a satisfactory computational performance when the accurate model of combined-cycle units is included in the traditional thermal unit commitment model.

In most circumstances, U.S. ISOs reduce the computational burden to solve a problem by reducing the accuracy of the combined-cycle unit model. This is the reason why current U.S. ISOs use an aggregated model or a pseudo unit approach to formulate the combined-cycle units [3]. However, these two modeling approaches oversimplify the coupling relationships among CTs and STs in a combined-cycle unit. For instance, the aggregated model uses a traditional thermal unit commitment model to represent the whole combined-cycle unit by ignoring the relationships among CTs and STs. Although the pseudo unit approach makes progress by considering the generation amount relationships among STs and CTs, this approach cannot capture the transition process of the combinations of CTs and STs [4]. As a result, these less accurate models bring challenges to the feasibility of operations. For example, prohibited transitions may appear in the optimal solutions obtained by the aggregated model and pseudo unit approaches. Therefore, some ISOs start to develop a configuration-based modeling approach (see, e.g., the pioneer works in [5] and [6] for the dynamic programming and MILP formulations) which can clearly describe the transition process of combined-cycle units among different modes (configurations). CAISO and ERCOT have implemented the configuration-based model in their markets [7] and [8]. As compared to the aggregated model and pseudo unit approaches, the configuration-based model significantly increases the computational time to solve the integrated unit commitment problem including both combined-cycle and traditional thermal units [9]. Recently, research progress has been made in providing tight MIP formulations of configuration-based combined-cycle units (see [7] and [10]). However, the configuration-based model still faces challenges in terms of accuracy because this approach cannot capture the operating constraints and costs for each turbine, as indicated in [11].

In order to improve the computational performance and accuracy of the combined-cycle unit model, an edge-based model is proposed in [12] to provide an accurate model for the problem. This model tracks the operating status of each turbine by using arcs in the transition graph as decision variables in the mathematical programming formulation. These arcs can also clearly represent the transition relationships among CTs and STs. This new modeling framework can exactly describe the operating physical constraints including the min-up/-down time requirements and time dependent start-up costs of each CT and ST in a combined-cycle unit by tracking its start-up and shut-down processes.

In this paper, we focus on improving the computational efficiency. More specifically, we improve the computational performance by taking advantage of the characteristics of current commercial MILP solvers, such as CPLEX, and the special structure of the transition graph for the problem. MILP solvers have been used to solve unit commitment problems by ISOs in the U.S. [13]. Following the branch-and-bound framework, advanced MILP solvers introduce cutting plane approaches, heuristic strategies, and presolve techniques [14] to solve the problem more quickly. Recent research progress in new techniques makes advanced MILP solvers a breakthrough to quickly solve large-sized problems.

Most MILP solvers implement the branch-and-bound algorithm associated with the linear programming (LP) relaxation at each branching node, including the root node. The optimal values of these LP relaxation problems at each node are important performance indicators for the solvers. Based on current LP relaxation optimal value and feasible integer solutions, the solvers decide the heuristic and branching strategies. In addition, the root-node LP relaxation has a significant impact on the choice of heuristic strategies and cutting planes. For a minimization MILP problem, a better root-node LP relaxation, which usually corresponds to a tighter MILP formulation, can provide a better lower bound, which helps obtain a better solution in a short time during the branch-and-bound process. Significant research progress has been made on how to strengthen the traditional thermal unit commitment formulation. For instance in [15], a classic MILP formulation is developed with three binary variables (start-up, shut-down, and the unit status). In [16], the min-up/-down time polytope based on two binary variables is strengthened. In [17], a computationally efficient MILP formulation with a single binary variable for each unit status is proposed. Recently, in [18] perspective cuts are proposed to approximate the quadratic generation cost curve. In [13], a tight unit commitment formulation is studied by the polyhedral approximation of the perspective reformulation. In [19], several families of strong valid ramping rate inequalities are derived to tighten the formulation. Furthermore in [20], a new set of decision variables is introduced to form a tight formulation.

Moving in a similar direction, we strengthen the edge-based formulation for combined-cycle units to improve its computational performance. We summarize our contributions as follows:

1) We derive tighter min-up/-down and ramping rate constraints for the edge-based combined-cycle unit model.
2) We provide several families of strong valid inequalities in terms of ramping rates for a combined-cycle unit by exploring the special structure of the transition graph of the problem. We show that the inequalities are valid for the whole problem and facet-defining under mild conditions.
3) We conduct computational experiments on different data sets, which verify the effectiveness of our proposed formulation.

The remaining part of our paper is organized as follows. In Section III, we describe the original edge-based formulation. In Section IV, we describe and explain our innovative tighter constraints and strong valid inequalities for combined-cycle units. In Section V we report and analyze our computational results. Finally, we conclude this study in Section VI.

## III. Edge-Based Formulation of a Combined-Cycle Unit

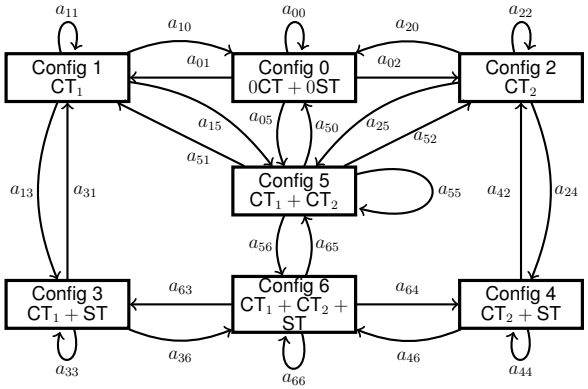


Fig. 1. Configuration Transition Graph

In this section, we first introduce the basic principle of edge-based formulation for combined-cycle units as described in [12]. Then we summarize the mathematical formulation of the edge-based formulation of a combined-cycle unit.

Fig. 1 displays all possible combinations of CTs and STs (i.e., configurations) and related transitions among different configurations in a combined-cycle unit with 2 CTs and 1 ST, which works on one of the configurations at each time period. In the edge-based formulation, each configuration is considered as a pseudo thermal unit, and each transition arc in the graph is designed corresponding to a decision variable to track the transition process within a combined-cycle unit. This edge-based formulation can be summarized as follows:

$$\sum_{a\in(\mathcal{A}_k^{\text{in}}\bigcup\mathcal{A}_k^{\text{sl}})} z_t^a = \sum_{a\in(\mathcal{A}_k^{\text{out}}\bigcup\mathcal{A}_k^{\text{sl}})} z_{t+1}^a, \forall k\in\mathcal{C},\forall t, \tag{1}$$

$$oc = \sum_{t\in\mathcal{T}}(pc_t + sc_t), \tag{2}$$

$$pc_t = \sum_{k\in\mathcal{C}} pc_t^k, \forall t, \tag{3}$$

$$sc_t = \sum_{i\in\mathcal{U}^{\text{CT}}}(su_t^i + sd_t^i), \forall t, \tag{4}$$

$$sd_t^i = \text{SDC}_i \sum_{a\in\mathcal{A}_i^{\text{sd}}} z_t^a, \forall i\in\mathcal{U}^{\text{CT}},\forall t, \tag{5}$$

$$su_t^i \geq \text{SUC}_{\text{hot}}^i \sum_{a\in\mathcal{A}_i^{\text{su}}} z_t^a, \forall i\in\mathcal{U}^{\text{CT}},\forall t, \tag{6}$$

$$su_t^i \geq \text{SUC}_{\text{warm}}^i\Big(\sum_{a\in\mathcal{A}_i^{\text{su}}} z_t^a - \sum_{\tau=T_{\text{md}}^i+1}^{T_{\text{warm}}^i}\sum_{a\in\mathcal{A}_{\text{sd}}^i} z_{t-\tau}^a\Big),$$
$$\forall i\in\mathcal{U}^{\text{CT}},\forall t, \tag{7}$$

$$su_t^i \geq \text{SUC}_{\text{cold}}^i\Big(\sum_{a\in\mathcal{A}_i^{\text{su}}} z_t^a - \sum_{\tau=T_{\text{md}}^i+1}^{T_{\text{cold}}^i}\sum_{a\in\mathcal{A}_{\text{sd}}^i} z_{t-\tau}^a\Big),$$
$$\forall i\in\mathcal{U}^{\text{CT}},\forall t, \tag{8}$$

$$\sum_{a\in\bigcup_{k\in\mathcal{C}_i^{\text{off}}}\mathcal{A}_k^{\text{all}}} z_\tau^a \leq 1 - \sum_{a\in\mathcal{A}_i^{\text{su}}} z_t^a, \forall i\in\mathcal{U}^{\text{CT}}\cup\mathcal{U}^{\text{ST}},$$
$$\forall\tau\in\{t+1,\cdots,\min\{\mathcal{T}_{\text{end}}, T_{\text{mu}}^i+t-1\}\},\forall t, \tag{9}$$

$$\sum_{a\in\bigcup_{k\in\mathcal{C}_i^{\text{on}}}\mathcal{A}_k^{\text{all}}} z_\tau^a \leq 1 - \sum_{a\in\mathcal{A}_i^{\text{sd}}} z_t^a, \forall i\in\mathcal{U}^{\text{CT}}\cup\mathcal{U}^{\text{ST}},$$
$$\tau\in\{t+1,\cdots,\min\{\mathcal{T}_{\text{end}}, T_{\text{md}}^i+t-1\}\},\forall t, \tag{10}$$

$$p_t = \sum_{k\in\mathcal{C}} p_t^k, \forall t, \tag{11}$$

$$\underline{P}_k\Big(\sum_{a\in(\mathcal{A}_k^{\text{in}}\bigcup\mathcal{A}_k^{\text{sl}})} z_t^a\Big) \leq p_t^k, \forall k\in\mathcal{C},\forall t, \tag{12}$$

$$p_t^k \leq \bar{P}_k\Big(\sum_{a\in(\mathcal{A}_k^{\text{in}}\bigcup\mathcal{A}_k^{\text{sl}})} z_t^a\Big), \forall k\in\mathcal{C},\forall t, \tag{13}$$

$$p_t + sr_t \leq \sum_{k\in\mathcal{C}}\bar{P}_k\Big(\sum_{a\in(\mathcal{A}_k^{\text{in}}\bigcup\mathcal{A}_k^{\text{sl}})} z_t^a\Big), \forall t, \tag{14}$$

$$sr_t \leq \sum_{k\in\mathcal{C}} 10R_k^{\text{MS}}\Big(\sum_{a\in(\mathcal{A}_k^{\text{in}}\bigcup\mathcal{A}_k^{\text{sl}})} z_t^a\Big), \forall t, \tag{15}$$

$$or_t - sr_t \leq P_{\text{QS}}\Big(\sum_{a\in(\mathcal{A}_k^{\text{in}}\bigcup\mathcal{A}_k^{\text{sl}})} z_t^a\Big), k=0,\forall t, \tag{16}$$

$$p_{t+1} - p_t \leq \text{RU}_a z_{t+1}^a + M(1-z_{t+1}^a), \forall a\in\mathcal{A},\forall t, \tag{17}$$

$$p_t - p_{t+1} \leq \text{RD}_a z_{t+1}^a + M(1-z_{t+1}^a), \forall a\in\mathcal{A},\forall t. \tag{18}$$

By considering the initial stage of the combined-cycle unit, logical constraints (1) keep tracking the transition process corresponding to each time period $t$ and configuration $k$. Constraint (2) describes the operating cost of a combined-cycle unit, which includes the production and transition costs. Constraints (3) indicate that the production cost is the sum of the production costs corresponding to each configuration since the combined-cycle unit works on only one configuration at each time period. Note here that typically $pc_t^k$ is a nondecreasing quadratic function, which can be approximated by a piecewise linear function. Constraints (4) describe the transition cost at each time period, which is equal to the sum of the start-up and shut-down costs of a combined-cycle unit. More specifically, the shut-down costs are described in constraints (5). The time dependent start-up costs are described in constraints (6) - (8) with the assumption that $\text{SUC}_{\text{hot}}^i < \text{SUC}_{\text{warm}}^i < \text{SUC}_{\text{cold}}^i$. Constraints (9) and (10) enforce the min-up/-down time requirements for each turbine in a combined-cycle unit respectively. Since each configuration is a pseudo thermal unit, the operating restrictions of these pseudo thermal units are represented in constraints (11) - (13). Equations (11) provide the representation of the generation amount of a combined-cycle unit. Constraints (12) and (13) restrict the generation amount of each configuration from below and above respectively. Constraints (14) - (16) describe the spinning reserve and operating reserve requirements for a combined-cycle unit. Finally, constraints (17) and (18)

describe ramping up/down rate restrictions. The $M$ in each of these constraints is equal to the capacity of the combined-cycle unit ($\bar{P}^{\text{c}}$).

Finally by considering the initial status of the combined-cycle unit, it is easy to observe that all arcs in the transition graph have the following relationship, which are implied by constraints (1).

$$\sum_{a\in\mathcal{A}} z_t^a = 1, \forall t. \tag{19}$$

## IV. Strengthened Formulation

In this section, we first explore the relationship between the statuses of the units and the transition graph. Then, we derive tighter constraints and several families of strong valid inequalities to improve the computational efficiency to solve the problem.

### A. Transition Statuses of Units

In the edge-based formulation, we use the edge variables to track the states of each turbine. As we know, each turbine has four transition statuses, which are start-up, shut-down, keeping on-line, and keeping off-line. Accordingly, all these edges can be divided into four groups for each turbine. We use $\text{CT}_1$ as an example to explain these four groups as shown in Fig.2. The dash dotted edges represent the shut-down process of turbine $\text{CT}_1$. The dash edges represent the start-up process of turbine $\text{CT}_1$. The solid edges represent $\text{CT}_1$ keeps online. The dotted edges represent $\text{CT}_1$ keeps offline. Mathematically, these four groups have the following relationships as shown in (20) - (23).

$$\begin{aligned}&\emptyset = \mathcal{A}_i^\kappa \cap \mathcal{A}_i^\tau, \forall \kappa, \tau \in \{\text{su}, \text{sd}, \text{on}, \text{off}\},\\ &\kappa \neq \tau, \forall i \in \mathcal{U}^{\text{CT}} \cup \mathcal{U}^{\text{ST}}.\end{aligned} \tag{20}$$

$$\mathcal{A} = \mathcal{A}_i^{\text{su}} \cup \mathcal{A}_i^{\text{sd}} \cup \mathcal{A}_i^{\text{on}} \cup \mathcal{A}_i^{\text{off}}, \forall i \in \mathcal{U}^{\text{CT}} \cup \mathcal{U}^{\text{ST}} \tag{21}$$

$$\bigcup_{k\in\mathcal{C}_i^{\text{off}}} \mathcal{A}_k^{\text{all}} = \mathcal{A}_i^{\text{su}} \cup \mathcal{A}_i^{\text{sd}} \cup \mathcal{A}_i^{\text{off}}, \forall i \in \mathcal{U}^{\text{CT}} \cup \mathcal{U}^{\text{ST}} \tag{22}$$

$$\bigcup_{k\in\mathcal{C}_i^{\text{on}}} \mathcal{A}_k^{\text{all}} = \mathcal{A}_i^{\text{su}} \cup \mathcal{A}_i^{\text{sd}} \cup \mathcal{A}_i^{\text{on}}, \forall i \in \mathcal{U}^{\text{CT}} \cup \mathcal{U}^{\text{ST}} \tag{23}$$

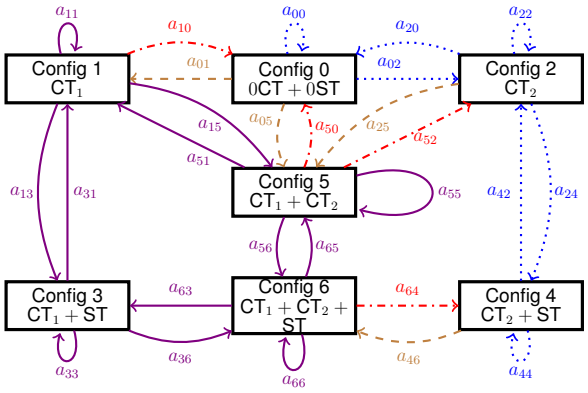


Fig. 2. Divided Groups

### B. Tighter Constraints

#### 1) Min-up Time Constraints:

$$\sum_{\kappa=1}^{T_{\text{mu}}^i-1} \sum_{a\in\mathcal{A}_i^{\text{su}}} z_{t-\kappa}^a \le 1 - \sum_{a\in\bigcup_{k\in\mathcal{C}_i^{\text{off}}}\mathcal{A}_k^{\text{all}}} z_t^a, \tag{24}$$
$$\forall i \in \mathcal{U}^{\text{CT}} \cup \mathcal{U}^{\text{ST}}, \forall t \in \{T_{\text{mu}}^i, \cdots, \mathcal{T}_{\text{end}}\}.$$

Motivated by the logic developed by [16] for the traditional thermal generation units, we develop tighter minimum up requirement constraints for each turbine in a combined-cycle unit as shown in (24). This logic can be described as that if turbine $i$ is online at time period $t$, then this turbine starts up at most once during time interval $[t - T_{\text{mu}}^i + 1, t - 1]$. In other words, if turbine $i$ starts up at time interval $[t-T_{\text{mu}}^i+1, t-1]$, then the configurations without turbine $i$ cannot be online at time period $t$. In the transition graph, if one of the arcs in $\mathcal{A}_i^{\text{su}}$, representing the start-up process of turbine $i$, is active during time interval $[t - T_{\text{mu}}^i + 1, t - 1]$, then arcs $\bigcup_{k\in\mathcal{C}_i^{\text{off}}} \mathcal{A}_k^{\text{all}}$ connected to the configurations ($\mathcal{C}_i^{\text{off}}$) without turbine $i$ cannot be active. In the following part, we show that constraints (24) are tighter than constraints (9).

To begin with, we rewrite constraints (9) as follows:

$$\sum_{a\in\mathcal{A}_i^{\text{su}}} z_s^a \le 1 - \sum_{a\in\bigcup_{k\in\mathcal{C}_i^{\text{off}}}\mathcal{A}_k^{\text{all}}} z_\tau^a, \forall i \in \mathcal{U}^{\text{CT}} \cup \mathcal{U}^{\text{ST}}, \tag{25}$$
$$\forall \tau \in \{s+1, \cdots, \min\{\mathcal{T}_{\text{end}}, T_{\text{mu}}^i + s - 1\}\}, \forall s \in \mathcal{T}.$$

By introducing $\kappa \in \{1, \cdots, T_{\text{mu}}^i - 1\}$, we reformulate constraints (25) as (26).

$$\sum_{e\in\mathcal{A}_i^{\text{su}}} z_s^e \le 1 - \sum_{e\in\bigcup_{k\in\mathcal{C}_i^{\text{off}}}\mathcal{A}_k^{\text{all}}} z_{s+\kappa}^e, \forall i \in \mathcal{U}^{\text{CT}} \cup \mathcal{U}^{\text{ST}}, \tag{26}$$
$$\forall \kappa \in \{1, \cdots, T_{\text{mu}}^i - 1\}, s + \kappa \le \mathcal{T}_{\text{end}}, \forall s \in \mathcal{T}.$$

Then, we replace $s + \kappa$ with $t$ to obtain (27).

$$\sum_{e\in\mathcal{A}_i^{\text{su}}} z_{t-\kappa}^e \le 1 - \sum_{e\in\bigcup_{k\in\mathcal{C}_i^{\text{off}}}\mathcal{A}_k^{\text{all}}} z_t^e, \forall i \in \mathcal{U}^{\text{CT}} \cup \mathcal{U}^{\text{ST}}, \tag{27}$$
$$\forall \kappa \in \{1, \cdots, T_{\text{mu}}^i - 1\}, t - \kappa \ge 1, \forall t \in \{2, \cdots, \mathcal{T}_{\text{end}}\}.$$

Therefore, we only need to show inequalities (24) are tighter than inequalities (27) in the following two cases.

First, we consider $t \in \{T_{\text{mu}}^i, \cdots, \mathcal{T}_{\text{end}}\}$. Then we can remove the condition $t - \kappa \ge 1$ and obtain (28) from (27) as follows.

$$\sum_{e\in\mathcal{A}_i^{\text{su}}} z_{t-\kappa}^e \le 1 - \sum_{e\in\bigcup_{k\in\mathcal{C}_i^{\text{off}}}\mathcal{A}_k^{\text{all}}} z_t^e, \forall i \in \mathcal{U}^{\text{CT}} \cup \mathcal{U}^{\text{ST}}, \tag{28}$$
$$\forall \kappa \in \{1, \cdots, T_{\text{mu}}^i - 1\}, \forall t \in \{T_{\text{mu}}^i, \cdots, \mathcal{T}_{\text{end}}\}.$$

It is easy to observe that constraints (28) are dominated by constraints (24).

Next, we consider $t \in \{2, T_{\text{mu}}^i - 1\}$. Note here that (27) can be rewritten as follows.

$$\sum_{e\in\mathcal{A}_i^{\text{su}}} z_{t-\kappa}^e \le 1 - \sum_{e\in\bigcup_{k\in\mathcal{C}_i^{\text{off}}}\mathcal{A}_k^{\text{all}}} z_t^e, \forall i \in \mathcal{U}^{\text{CT}} \cup \mathcal{U}^{\text{ST}}, \tag{29}$$
$$\forall \kappa \in \{1, \cdots, t-1\}, \forall t \in \{2, T_{\text{mu}}^i - 1\}.$$

In constraints (29), we can have $\kappa \in \{1, \cdots, t-1\}$ due to $t-1 < T^i_{\text{mu}} - 1$ and $\kappa \leq t-1$. Then, it is easy to check that constraints (29) are dominated by (30), which are equivalent to (31).

$$\sum_{\kappa=1}^{t-1} \sum_{e \in \mathcal{A}_i^{\text{su}}} z^e_{t-\kappa} \leq 1 - \sum_{e \in \bigcup_{k \in \mathcal{C}_i^{\text{off}}} \mathcal{A}_k^{\text{all}}} z^e_t, \forall i \in \mathcal{U}^{\text{CT}} \cup \mathcal{U}^{\text{ST}}, \quad (30)$$
$$\forall t \in \{2, T^i_{\text{mu}} - 1\}.$$
$$\sum_{\omega=1}^{t-1} \sum_{e \in \mathcal{A}_i^{\text{su}}} z^e_{\omega} \leq 1 - \sum_{e \in \bigcup_{k \in \mathcal{C}_i^{\text{off}}} \mathcal{A}_k^{\text{all}}} z^e_t, \forall i \in \mathcal{U}^{\text{CT}} \cup \mathcal{U}^{\text{ST}}, \quad (31)$$
$$\forall t \in \{2, T^i_{\text{mu}} - 1\}.$$

Now we show an equivalent formulation of constraints (31) is dominated by (24). To that end, we first rewrite the left hand side (LHS) of constraints (31) by using the following logic relationship as shown in constraints (32), which are further equivalent to (33) by taking summation over $\omega \in [2, t]$.

$$\sum_{e \in \mathcal{A}_i^{\text{su} \cup \text{on}}} z^e_{t+1} - \sum_{e \in \mathcal{A}_i^{\text{su} \cup \text{on}}} z^e_t + \sum_{e \in \mathcal{A}_i^{\text{sd}}} z^e_{t+1} = \sum_{e \in \mathcal{A}_i^{\text{su}}} z^e_{t+1},$$
$$\forall t \in \mathcal{T}, \forall i \in \mathcal{U}^{\text{CT}} \cup \mathcal{U}^{\text{ST}}. \quad (32)$$
$$\sum_{\omega=2}^{t} \sum_{e \in \mathcal{A}_i^{\text{su}}} z^e_{\omega} = \sum_{e \in \mathcal{A}_i^{\text{su} \cup \text{on}}} z^e_t - \sum_{e \in \mathcal{A}_i^{\text{su} \cup \text{on}}} z^e_1 + \sum_{\omega=2}^{t} \sum_{e \in \mathcal{A}_i^{\text{sd}}} z^e_{\omega}$$
$$\forall t \in \mathcal{T}, \forall i \in \mathcal{U}^{\text{CT}} \cup \mathcal{U}^{\text{ST}} \quad (33)$$
$$\sum_{\omega=1}^{t} \sum_{e \in \mathcal{A}_i^{\text{su}}} z^e_{\omega} = \sum_{e \in \mathcal{A}_i^{\text{su} \cup \text{on}}} z^e_t - \sum_{e \in \mathcal{A}_i^{\text{on}}} z^e_1 + \sum_{\omega=2}^{t} \sum_{e \in \mathcal{A}_i^{\text{sd}}} z^e_{\omega}$$
$$\forall t \in \mathcal{T}, \forall i \in \mathcal{U}^{\text{CT}} \cup \mathcal{U}^{\text{ST}} \quad (34)$$

By moving the item $\sum_{e \in \mathcal{A}_i^{\text{su}}} z^e_1$ to the LHS of constraints (33), we obtain (34). Therefore, we can reformulate constraints (31) as constraints (35) at given time period $t$ by moving the item $\sum_{e \in \mathcal{A}_i^{\text{su}}} z^e_t$ in (31) to the LHS based on the relationships indicated by constraints (22). Furthermore, we can rewrite constraints (35) as (36) by using constraints (34).

$$\sum_{\omega=1}^{t} \sum_{e \in \mathcal{A}_i^{\text{su}}} z^e_{\omega} \leq 1 - \sum_{e \in \mathcal{A}_i^{\text{sd}} \cup \mathcal{A}_i^{\text{off}}} z^e_t,$$
$$\forall t \in \{2, T^i_{\text{mu}} - 1\}, \forall i \in \mathcal{U}^{\text{CT}} \cup \mathcal{U}^{\text{ST}}, \quad (35)$$
$$\sum_{e \in \mathcal{A}_i^{\text{su} \cup \text{on}}} z^e_t - \sum_{e \in \mathcal{A}_i^{\text{su} \cup \text{on}}} z^e_1 + \sum_{\omega=2}^{t} \sum_{e \in \mathcal{A}_i^{\text{sd}}} z^e_{\omega} \leq 1 - \sum_{e \in \mathcal{A}_i^{\text{sd}} \cup \mathcal{A}_i^{\text{off}}} z^e_t,$$
$$\forall t \in \{2, T^i_{\text{mu}} - 1\}, \forall i \in \mathcal{U}^{\text{CT}} \cup \mathcal{U}^{\text{ST}}. \quad (36)$$

Based on (19) and (21), we can observe that constraints (36) are equivalent to constraints (37).

$$\sum_{\omega=2}^{t} \sum_{e \in \mathcal{A}_i^{\text{sd}}} z^e_{\omega} \leq \sum_{e \in \mathcal{A}_i^{\text{su} \cup \text{on}}} z^e_1$$
$$\forall t \in \{2, T^i_{\text{mu}} - 1\}, \forall i \in \mathcal{U}^{\text{CT}} \cup \mathcal{U}^{\text{ST}}. \quad (37)$$

By following the similar process to obtain constraints (37), we get an equivalent formulation (38) of constraints (24) when $t = T^i_{\text{mu}}$. Obviously, the constraints in (37) at given time period $t \in \{2, T^i_{\text{mu}} - 1\}$ are dominated by constraints (38).

$$\sum_{\omega=2}^{T^i_{\text{mu}}} \sum_{e \in \mathcal{A}_i^{\text{sd}}} z^e_{\omega} \leq \sum_{e \in \mathcal{A}_i^{\text{su} \cup \text{on}}} z^e_1, \forall i \in \mathcal{U}^{\text{CT}} \cup \mathcal{U}^{\text{ST}}. \quad (38)$$

Hence, we finished the proof by discussing two cases.

*2) Min-down Time Constraints:* We can formulate tighter constraints for min-down time requirements following the similar idea as the reformulation of minimum up time requirement constraints.

$$\sum_{\kappa=1}^{T^i_{\text{md}}-1} \sum_{a \in \mathcal{A}_i^{\text{sd}}} z^a_{t-\kappa} \leq 1 - \sum_{a \in \bigcup_{k \in \mathcal{C}_i^{\text{on}}} \mathcal{A}_k^{\text{all}}} z^a_t,$$
$$\forall i \in \mathcal{U}^{\text{CT}} \cup \mathcal{U}^{\text{ST}}, \forall t \in \{T^i_{\text{md}}, \cdots, \mathcal{T}_{\text{end}}\}. \quad (39)$$

Constraints (39) indicate that if one of the arcs in $\mathcal{A}^i_{\text{sd}}$, representing the shut-down process of turbine $i$, is active during time interval $[t - T^i_{\text{md}} + 1, t-1]$, then arcs $\bigcup_{k \in \mathcal{C}_i^{\text{on}}} \mathcal{A}_k^{\text{all}}$ connected to the configurations ($\mathcal{C}_i^{\text{on}}$) with turbine $i$ cannot be active. This means the configurations with turbine $i$ must be offline at time period $t$ when turbine $i$ shuts down at time interval $[t - T^i_{\text{md}} + 1, t-1]$. Similarly, following the arguments as described in the previous part, we can observe that constraints (39) are tighter than constraints (10).

*3) Ramping Rate Constraints:* As mentioned previously, the edge-based formulation tracks the transition process of a combined-cycle unit by recording the status of each arc. The status of each arc indicates the operating status of the combined-cycle unit, which further determines which ramping rate limit (corresponding to each arc) affects the change of the generation amount at each time period. Hence, ramping rate constraints (17) and (18) use the arc decision variables to make the choice of ramping rate limits. Instead of using big-M, we propose the following ramping rate constraints (40) and (41).

$$p_{t+1} - p_t \leq \sum_{a \in \mathcal{A}} \text{RU}_a z^a_{t+1}, \forall t \in \mathcal{T}, \quad (40)$$
$$p_t - p_{t+1} \leq \sum_{a \in \mathcal{A}} \text{RD}_a z^a_{t+1}, \forall t \in \mathcal{T}. \quad (41)$$

Because only one of the arcs in the transition graph can be active at each time period $t$ as shown in (19), only one item in the right-hand side of (40) can be positive and all others would be zero. This positive item represents the active arc that provides the ramping up rate limit. The same analysis can be applied to ramping down constraints (41).

By considering constraints (19) and the fact that $M \geq \max\{\text{RU}_a, \text{RD}_a\}, \forall a$, it is easy to check that constraints (40) and (41) dominate constraints (17) and (18), respectively.

Next, we show that inequality (40) is facet-defining for the projection of the whole feasible space (denoted as $\mathcal{Q}$) onto $\mathcal{S} = \{z^a_{t+1}, p_{t+1}, p_t \ \forall a \in \mathcal{A}\}$ when $\underline{P}_n \leq \underline{P}_m + \text{RU}_{m,n} \leq \bar{P}_n$. As there are $|\mathcal{A}|+2$ variables and $\sum_{a \in \mathcal{A}} z^a_{t+1} = 1$, the dimension of $\mathcal{S}$ is $|\mathcal{A}|+1$. In order to prove that inequality (40) is facet-defining for $\mathcal{S}$, we need $|\mathcal{A}|+1$ affinely independent points which satisfy $p_{t+1} - p_t = \sum_{a \in \mathcal{A}} \text{RU}_a z^a_{t+1}$ at time period $t+1$ as shown in Table I. Similarly, we can show inequality (41) is facet-defining for the space $S$ under mild conditions.

TABLE I
$|\mathcal{A}|+1$ AFFINELY INDEPENDENT POINTS

| Arc | $z^a_{t+1}$ | | | | | $p_{t+1}$ | $p_t$ |
|---|---|---|---|---|---|---|---|
| | $a(m_1,n_1)$ | $a(m_2,n_2)$ | $\ddots$ | $a(m_{\lvert\mathcal{A}\rvert-1},n_{\lvert\mathcal{A}\rvert-1})$ | $a(m_{\lvert\mathcal{A}\rvert},n_{\mathcal{A}})$ | | |
| $(m_1,n_1)$ | 1 | 0 | 0 | 0 | 0 | $\underline{P}_{m_1}+\text{RU}_{a(m_1,n_1)}$ | $\underline{P}_{m_1}$ |
| $(m_2,n_2)$ | 0 | 1 | 0 | 0 | 0 | $\underline{P}_{m_2}+\text{RU}_{a(m_2,n_2)}$ | $\underline{P}_{m_2}$ |
| $\ddots$ | 0 | 0 | $\ddots$ | 0 | 0 | $\ddots$ | $\ddots$ |
| $(m_{\lvert\mathcal{A}\rvert-1},n_{\lvert\mathcal{A}\rvert-1})$ | 0 | 0 | 0 | 1 | 0 | $\underline{P}_{m_{\lvert\mathcal{A}\rvert-1}}+\text{RU}_{a(m_{\lvert\mathcal{A}\rvert-1},n_{\lvert\mathcal{A}\rvert-1})}$ | $\underline{P}_{m_{\lvert\mathcal{A}\rvert-1}}$ |
| $(m_{\lvert\mathcal{A}\rvert},n_{\mathcal{A}})$ | 0 | 0 | 0 | 0 | 1 | $\underline{P}_{m_{\lvert\mathcal{A}\rvert}}+\text{RU}_{a(m_{\lvert\mathcal{A}\rvert},n_{\lvert\mathcal{A}\rvert})}$ | $\underline{P}_{m_{\lvert\mathcal{A}\rvert}}$ |
| $(m_1,n_1)$ | 1 | 0 | 0 | 0 | 0 | $\underline{P}_{m_1}+\text{RU}_{a(m_1,n_1)}+\epsilon$ | $\underline{P}_{m_1}+\epsilon$ |

### C. Strong Valid Inequalities

*1) Single-Arc Ramping Rate Inequalities:* In the previous section, inequalities (40) and (41) focus on the change of generation amount $p_t$ for the whole combined-cycle unit. Notice that equations (11) indicate that only the online configuration of the combined-cycle unit provides the generation amount. Now, we focus on the change of generation amount $p^k_t$ at each configuration of the combined-cycle unit. Given a specific arc $a(n,m)$, the combined-cycle unit transitions from Configurations $n$ to $m$. Accordingly, we focus on ramping rates and propose strong valid inequalities corresponding to this arc $a(n,m)$, named single-arc ramping rate inequalities as follows:

$$p^m_{t+1}-p^n_t \le \text{RU}^{a(n,m)} z^{a(n,m)}_{t+1} + \bar{P}_m\Big(\sum_{a\in(\mathcal{A}^{\text{in}}_m \bigcup \mathcal{A}^{\text{sl}}_m)} z^a_{t+1}\Big) - \underline{P}_n\Big(\sum_{a\in(\mathcal{A}^{\text{in}}_n \bigcup \mathcal{A}^{\text{sl}}_n)} z^a_t\Big) + (\underline{P}_n-\bar{P}_m) z^{a(n,m)}_{t+1}, \quad \forall a(n,m)\in\mathcal{A}, \forall t\in\mathcal{T}, \tag{42}$$

$$p^n_t-p^m_{t+1} \le \text{RD}^{a(n,m)} z^{a(n,m)}_{t+1} + \bar{P}_n\Big(\sum_{a\in(\mathcal{A}^{\text{in}}_n \bigcup \mathcal{A}^{\text{sl}}_n)} z^a_t\Big) - \underline{P}_m\Big(\sum_{a\in(\mathcal{A}^{\text{in}}_m \bigcup \mathcal{A}^{\text{sl}}_m)} z^a_{t+1}\Big) + (\underline{P}_m-\bar{P}_n) z^{a(n,m)}_{t+1}, \quad \forall a(n,m)\in\mathcal{A}, \forall t\in\mathcal{T}. \tag{43}$$

Note here that it is not necessary to distinguish Configuration $n$ from Configuration $m$ in both inequalities (42) and (43). When $n=m$, it means the combined-cycle unit keeps working on one configuration, where the ramping rate is within the corresponding configuration. When $n\neq m$, it means the combined-cycle unit transitions from one configuration to another. In this case, the ramping rate is between these two configurations.

First, we show the validity of ramping up inequalities (42) for a given arc $a(n,m)$ by discussing four possible cases as follows.

Case 1: the combined-cycle unit works on Configuration $n$ at time period $t$ and works on Configuration $m$ at time period $t+1$. It follows that arc $a(n,m)$ is active at $t+1$ in this case, and the ramping rate limit corresponding to arc $a(n,m)$ is selected to limit the change of the generation amount of the combined-cycle unit from $t$ to $t+1$. Accordingly, we have $z^{a(n,m)}_{t+1}=1$, $\sum_{a\in(\mathcal{A}^{\text{in}}_n \bigcup \mathcal{A}^{\text{sl}}_n)} z^a_t=1$, and $\sum_{a\in(\mathcal{A}^{\text{in}}_m \bigcup \mathcal{A}^{\text{sl}}_m)} z^a_{t+1}=1$. Then inequalities (42) convert to $p^m_{t+1}-p^n_t \le \text{RU}^{a(n,m)}$, which is valid due to constraints (17).

Case 2: the combined-cycle unit works on Configuration $n$ at time period $t$ and does not work on Configuration $m$ at time period $t+1$. It follows that arc $a(n,m)$ is not active at time period $t+1$ in this case, and the ramping rate limit corresponding to arc $a(n,m)$ will not be selected to limit the change of generation amount of the combined-cycle unit. Accordingly, we have $z^{a(n,m)}_{t+1}=0$, $\sum_{a\in(\mathcal{A}^{\text{in}}_n \bigcup \mathcal{A}^{\text{sl}}_n)} z^a_t=1$, and $\sum_{a\in(\mathcal{A}^{\text{in}}_m \bigcup \mathcal{A}^{\text{sl}}_m)} z^a_{t+1}=0$. Then inequalities (42) convert to $-p^n_t \le -\underline{P}_n$ which is valid due to constraints (12).

Case 3: the combined-cycle unit does not work on Configuration $n$ at time period $t$. However, it works on Configuration $m$ at time period $t+1$. Similar to Case 2, we have $z^{a(n,m)}_{t+1}=0$, $\sum_{a\in(\mathcal{A}^{\text{in}}_n \bigcup \mathcal{A}^{\text{sl}}_n)} z^a_t=0$, and $\sum_{a\in(\mathcal{A}^{\text{in}}_m \bigcup \mathcal{A}^{\text{sl}}_m)} z^a_{t+1}=1$ in this case. Then inequalities (42) become $p^m_{t+1}\le \bar{P}_m$, which is valid due to constraints (13).

Case 4: the combined-cycle unit neither works on Configuration $n$ at time period $t$, nor works on Configuration $m$ at time period $t+1$. It follows that we have $z^{a(n,m)}_{t+1}=0$, $\sum_{a\in(\mathcal{A}^{\text{in}}_n \bigcup \mathcal{A}^{\text{sl}}_n)} z^a_t=0$, and $\sum_{a\in(\mathcal{A}^{\text{in}}_m \bigcup \mathcal{A}^{\text{sl}}_m)} z^a_{t+1}=0$. Inequalities (42) become $0\le 0$.

These four cases cover all scenarios of inequalities (42) for a given arc $a(n,m)$. To make it clearer, we summarize this analysis in Table II. Similar analysis can be applied to inequalities (43) and is summarized in Table III.

TABLE II
VALIDITY OF RAMPING UP INEQUALITIES (42)

| Case | Value of Binary Variables | | | Inequality | |
|---|---|---|---|---|---|
| | $\sum_{a\in(\mathcal{A}^{\text{in}}_n \bigcup \mathcal{A}^{\text{sl}}_n)} z^a_t$ | $\sum_{a\in(\mathcal{A}^{\text{in}}_m \bigcup \mathcal{A}^{\text{sl}}_m)} z^a_{t+1}$ | $z^{a(n,m)}_{t+1}$ | LHS | RHS |
| 1 | 1 | 1 | 1 | $p^m_{t+1}-p^n_t$ | $\text{RU}^{a(n,m)}$ |
| 2 | 1 | 0 | 0 | $-p^n_t$ | $-\underline{P}_n$ |
| 3 | 0 | 1 | 0 | $p^m_{t+1}$ | $\bar{P}_m$ |
| 4 | 0 | 0 | 0 | 0 | 0 |

TABLE III
VALIDITY OF RAMPING DOWN INEQUALITIES (43)

| Case | Value of Binary Variables | | | Inequality | |
|---|---|---|---|---|---|
| | $\sum_{a\in(\mathcal{A}^{\text{in}}_n \bigcup \mathcal{A}^{\text{sl}}_n)} z^a_t$ | $\sum_{a\in(\mathcal{A}^{\text{in}}_m \bigcup \mathcal{A}^{\text{sl}}_m)} z^a_{t+1}$ | $z^{a(n,m)}_{t+1}$ | LHS | RHS |
| 1 | 1 | 1 | 1 | $p^n_t-p^m_{t+1}$ | $\text{RD}^{a(n,m)}$ |
| 2 | 1 | 0 | 0 | $p^n_t$ | $\bar{P}_n$ |
| 3 | 0 | 1 | 0 | $-p^m_{t+1}$ | $-\underline{P}_m$ |
| 4 | 0 | 0 | 0 | 0 | 0 |

Next, for each $(n,m)\in\mathcal{A}$ at $t+1$, we show inequality (42) is facet-defining for the projection of the whole feasible space (denoted as $\mathcal{Q}$) onto $\mathcal{S}=\{z^a_t, z^a_{t+1}, p^n_t, p^n_{t+1},\ \forall a\in\mathcal{A}\}$ when $\underline{P}_m \le \underline{P}_n+\text{RU}^{a(n,m)}<\bar{P}_m$ and $\bar{P}_m-\bar{P}_n<\text{RU}^{a(n,m)}$, $\forall(n,m)\in\mathcal{A}$, where $\mathcal{S}$ consists of all the variables describing inequality (42). As there are $2(|\mathcal{A}|+|\mathcal{C}|)$ variables in $\mathcal{S}$, $\sum_{a\in(\mathcal{A}^{\text{in}}_k \bigcup \mathcal{A}^{\text{sl}}_k)} z^a_t = \sum_{a\in(\mathcal{A}^{\text{out}}_k \bigcup \mathcal{A}^{\text{sl}}_k)} z^a_{t+1}, \forall k\in\mathcal{C}$, and $\sum_{a\in\mathcal{A}} z^a_t=1$, the dimension of the projection of $\mathcal{Q}$ onto $\mathcal{S}$ is

$2|\mathcal{A}|+|\mathcal{C}|-1$. In the following part, we show $2|\mathcal{A}|+|\mathcal{C}|-1$ affinely independent points which satisfy the equality of (42) to prove the facet-defining property. We let $\epsilon$ be an arbitrarily small positive number in the following part of this paper. As shown in Table IV, we divided these $2|\mathcal{A}|+|\mathcal{C}|-1$ points into 14 separated groups. Each row in this table represents a point satisfying equality and each column represents a variable. To better construct points regarding variable $z^a_{t+1}$, we divided the arc set $\mathcal{A}$ into 6 separated sets by giving arc $(n,m)$ as shown in (44). Similar, we divided the arc set $\mathcal{A}$ for variable $z^a_t$ as shown in (45). In this table, $I$ represents the identity matrix, $E$ represents the vector with 1 at each component. In addition, $E_1$ represents the vector with 1 at the first component and 0 at others. For given arc $(n,m)$, we construct these points as follows:

$$\begin{aligned}
&\mathcal{A} = \bar{\mathcal{A}}_1 \cup \bar{\mathcal{A}}_2 \cup \bar{\mathcal{A}}_3 \cup \bar{\mathcal{A}}_4 \cup \bar{\mathcal{A}}_5 \cup \bar{\mathcal{A}}_6 && (44)\\
&\bar{\mathcal{A}}_1 = \{(n,m)\}\\
&\bar{\mathcal{A}}_2 = \{(k,m), k \in \mathcal{C}_{\to m}, k \neq n\}\\
&\bar{\mathcal{A}}_3 = \{(n,s), s \in \mathcal{C}_{n\to}, s \neq m\}\\
&\bar{\mathcal{A}}_4 = \{(k,r), \forall k \in \mathcal{C}_{\to m}, k \neq n, \forall r \in \mathcal{C}_{k\to}, r \neq m\}\\
&\bar{\mathcal{A}}_5 = \{(x,x), x \in \mathcal{C}, x \neq n, x \neq k\}\\
&\bar{\mathcal{A}}_6 = \{(x,y), \forall y \in \mathcal{C}_{x\to}, x \neq n, x \neq k, y \neq x\}\\
&\mathcal{A} = \tilde{\mathcal{A}}_1 \cup \tilde{\mathcal{A}}_2 \cup \tilde{\mathcal{A}}_3 \cup \tilde{\mathcal{A}}_4 \cup \tilde{\mathcal{A}}_5 \cup \tilde{\mathcal{A}}_6 && (45)\\
&\tilde{\mathcal{A}}_1 = \{(n,n)\}\\
&\tilde{\mathcal{A}}_2 = \{(u,n), u \in \mathcal{C}_{\to n}, u \neq n\}\\
&\tilde{\mathcal{A}}_3 = \{(k,k), k \in \mathcal{C}_{\to m}, k \neq n\}\\
&\tilde{\mathcal{A}}_4 = \{(v,k), k \in \mathcal{C}_{\to m}, k \neq n, v \neq k, v \in \mathcal{C}_{\to k}\}\\
&\tilde{\mathcal{A}}_5 = \{(x,x), x \in \mathcal{C}, x \neq n, x \neq k\}\\
&\tilde{\mathcal{A}}_6 = \{(w,x), w \in \mathcal{C}_{\to x}, w \neq x, x \neq n, x \neq k\} && (46)
\end{aligned}$$

In Group 1, we construct one point based on the arc $(n,m)$ by letting $z^{a(n,m)}_{t+1}=1, z^{a(n,n)}_t=1, p^m_{t+1}=\underline{P}_n+\text{RU}^{a(n,m)}, p_t=\underline{P}_n$. In Group 2, we construct $|\mathcal{C}_{\to m}|-1$ points based on the incoming arcs of Configuration $m$ except the arc $(n,m)$ (i.e. $\bar{\mathcal{A}}_2$) by letting $z^{a(k,m)}_{t+1}=1, z^{a(k,k)}_t=1, p^m_{t+1}=\bar{P}^m, p^k_t=\bar{P}^m-\text{RU}^{a(k,m)}$ for each $k \in \mathcal{C}_{\to m}, k \neq m$. In Group 3, we let $z^{a(n,s)}_{t+1}=1, z^{a(n,n)}_t=1, p^s_{t+1}=\underline{P}_n+\text{RU}^{a(n,s)}, p^n_t=\underline{P}_n$ for each outgoing arc of Configuration $n$ except arc $(n,m)$(i.e. $\{\forall a \in \bar{\mathcal{A}}_3\}$), where $|\mathcal{C}_{n\to}|-1$ points are generated. In Group 4, we study the outgoing arcs of Configuration $k$, which can transition to Configuration $m$ except configuration $n$ as shown in $\bar{\mathcal{A}}_4$. Notice that arcs $(k,m)$ are not in the set $\bar{\mathcal{A}}_4$. Then, we generate $\sum_{k\in\mathcal{C}_{\to m},k\neq n}(|\mathcal{C}_{k\to}|-1)$ (i.e. $|\bar{\mathcal{A}}_4|$) points by letting $z^{a(k,r)}_{t+1}=1, z^{a(k,k)}_t=1, p^r_{t+1}=\underline{P}_k+\text{RU}^{a(k,r)}, p^k_t=\underline{P}_k$. In Group 5, we focus on the self-looping arcs for each configuration except the configurations which can transition to Configuration $m$ (i.e. $\bar{\mathcal{A}}_5$). Accordingly, $|\mathcal{C}|-|\mathcal{C}_{\to m}|$ points are constructed by letting $z^{a(x,x)}_{t+1}, z^{a(x,x)}_t=1, p^x_{t+1}=\underline{P}_x+\text{RU}^{a(x,x)}, p^x_t=\underline{P}_x$. Furthermore, we study the arcs in $\bar{\mathcal{A}}_6$. $|\mathcal{A}|-|\mathcal{C}|+1-\sum_{k\in\mathcal{C}_{\to m},k\neq n}(|\mathcal{C}_{k\to}|-1)-|\mathcal{C}_{n\to}|$ points are generated by letting $z^{a(x,y)}_{t+1}=1, z^{a(x,x)}_t=1, p^y_{t+1}=\underline{P}_x+\text{RU}^{a(x,y)}, p^x_t=\underline{P}_x$. From Group 1 to Group 6, we generated $|\mathcal{A}|$ points in total.

In Group 7, we construct one point similar to the point in Group 1 by letting $z^{a(n,m)}_{t+1}=1, z^{a(n,n)}_t=1, p^m_{t+1}=\underline{P}_n+\text{RU}^{a(n,m)}+\epsilon, p_t=\underline{P}_n+\epsilon$. In Group 8, we study the incoming arcs of Configuration $n$ except the arc $(n,n)$. $|\mathcal{C}_{\to n}|-1$ points are constructed by letting $z^{a(n,m)}_{t+1}=1, z^{a(u,n)}_t=1, p^m_{t+1}=\underline{P}_n+\text{RU}^{a(n,m)}, p_t=\underline{P}_n$. In Group 9, we construct $|\mathcal{C}_{\to m}|-1$ points by using the points in Group 2 as $z^{a(k,m)}_{t+1}=1, z^{a(k,k)}_t=1, p^m_{t+1}=\bar{P}^m, p^k_t=\bar{P}^m-\text{RU}^{a(k,m)}+\epsilon$. In Group 10, we continue studying the configurations $k$ which can transition to Configuration $m$. Here, we don't include Configuration $n$ and the self-looping arcs for Configuration $k$. We construct $\sum_{k\in\mathcal{C}_{\to m},k\neq n}(|\mathcal{C}_{\to k}|-1)$ points by letting $z^{(k,m)}_{t+1}=1, z^{(v,k)}_t=1, p^m_{t+1}=\bar{P}_m, p^k_t=\bar{P}_m-\text{RU}^{a(k,m)}$. In Group 11, we construct $|\mathcal{C}|-|\mathcal{C}_{\to m}|$ points by using the points in Group 5 as $z^{a(x,x)}_{t+1}, z^{a(x,x)}_t=1, p^x_{t+1}=\underline{P}_x+\text{RU}^{a(x,x)}+\epsilon, p^x_t=\underline{P}_x+\epsilon$. In Group 12, we study the arcs in $\tilde{\mathcal{A}}_6$. We construct $|\mathcal{A}|-|\mathcal{C}|+1-\sum_{k\in\mathcal{C}_{\to m},k\neq n}(|\mathcal{C}_{\to k}|-1)-|\mathcal{C}_{\to n}|$ points by letting $z^{a(x,x)}_{t+1}, z^{a(x,x)}_t=1, p^x_{t+1}=\underline{P}_x+\text{RU}^{a(x,x)}, p^x_t=\underline{P}_x$. From Group 7 - 12, we generate $\mathcal{A}$ points in total.

Now, we construct the last two group points. In Group 13, we construct $|\mathcal{C}|-|\mathcal{C}_{\to m}|$ points by letting $z^{a(x,x)}_{t+1}=1, z^{a(m_0,x)}_t=1, p^x_{t+1}=\underline{P}_x+\text{RU}^{a(x,x)}+\epsilon, p^x_t=\underline{P}_x+\epsilon$. In Group 14, we construct $|\mathcal{C}_{\to m}|-1$ points by letting $z^{(k,m)}_{t+1}=1, z^{(v,k)}_t=1, p^m_{t+1}=\bar{P}_m, p^k_t=\bar{P}_m-\text{RU}^{a(k,m)}+\epsilon$.

In summary, we have $2|\mathcal{A}|+|\mathcal{C}|-1$ affinely independent points satisfying the equality of (42). Similar process can be applied to inequality (43).

*2) Multi-Configuration Ramping Rate Inequalities:* In Subsection IV-C1, inequalities (42) and (43) study the ramping rate limits for a given arc. In this subsection, we extend the study to develop the ramping rate inequalities by considering a given configuration and its relationships with other configurations, named multi-configuration ramping rate inequalities.

Suppose that the combined-cycle unit works on Configuration $m$ at time period $t+1$. As shown in Fig. 3, we know one of the incoming arcs $(a_{n_1,m}, a_{n_2,m}, a_{n_3,m})$ or the self-loop arc $a_{m,m}$ must be active at time period $t+1$. On the other hand, suppose that the combined-cycle unit works on Configuration $n$ at time period $t$ in Fig. 4. Then, one of the outgoing arcs $(a_{n,m_1}, a_{n,m_2}, a_{n,m_3})$ or the self-loop arc $a_{n,n}$ must be active at time period $t+1$. We develop ramping rate inequalities for these two scenarios separately.

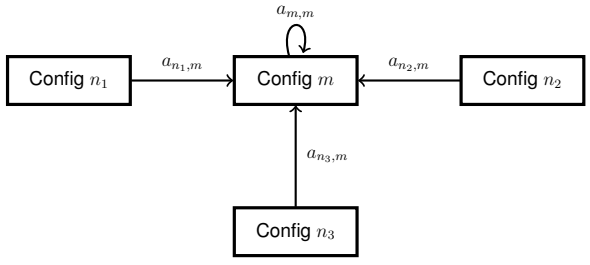


Fig. 3. Configuration Transition Graph for Configuration $m$

For the first scenario as shown in Fig. 3, the ramping

TABLE IV
$2|\mathcal{A}| + |\mathcal{C}| - 1$ AFFINELY INDEPENDENT POINTS FOR INEQUALITY (42)

| # Point | $z^a_{t+1}, \forall a \in \mathcal{A}$ | | | | | | $z^a_t, \forall a \in \mathcal{A}$ | | | | | | $p^c_{t+1}, \forall c \in \mathcal{C}$ | $p^c_t, \forall c \in \mathcal{C}$ |
|---|---|---|---|---|---|---|---|---|---|---|---|---|---|---|
| | $(n,m)$ | $(k,m)$<br>$k \in \mathcal{C}_{\to m}$<br>$k \neq n$ | $(n,s)$<br>$s \in \mathcal{C}_{n\to}$<br>$s \neq m$ | $(k,r)$<br>$\forall k \in \mathcal{C}_{\to m}$<br>$k \neq n$<br>$\forall r \in \mathcal{C}_{k\to}, r \neq m$ | $(x,x)$<br>$x \in \mathcal{C}$<br>$x \neq n$<br>$x \neq k$ | $(x,y)$<br>$\forall y \in \mathcal{C}_{x\to}$<br>$x \neq n, x \neq k$<br>$y \neq x$ | $(n,n)$ | $(u,n)$<br>$u \in \mathcal{C}_{\to n}$<br>$u \neq n$ | $(k,k)$<br>$k \in \mathcal{C}_{\to m}$<br>$k \neq n$ | $(v,k)$<br>$k \in \mathcal{C}_{\to m}$<br>$k \neq n, v \neq k$<br>$v \in \mathcal{C}_{\to k}$ | $(x,x)$<br>$x \in \mathcal{C}$<br>$x \neq n$<br>$x \neq k$ | $(w,x)$<br>$w \in \mathcal{C}_{\to x}$<br>$w \neq x$<br>$x \neq n, x \neq k$ | | |
| 1 | 1 | 0 | 0 | 0 | 0 | 0 | 1 | 0 | 0 | 0 | 0 | 0 | $p^{c=m}_{t+1} = \underline{P}_n + \mathrm{RU}^{a(n,m)}$<br>$p^c_{t+1} = 0, \forall c \in \mathcal{C}, c \neq m$ | $p^{c=n}_t = \underline{P}_n$<br>$p^c_t = 0, \forall c \in \mathcal{C}, c \neq n$ |
| $\lvert\mathcal{C}_{\to m}\rvert - 1$ | 0 | I | 0 | 0 | 0 | 0 | 0 | 0 | I | 0 | 0 | 0 | $p^{c=m}_{t+1} = \bar{P}_m$<br>$p^c_{t+1} = 0, \forall c \in \mathcal{C}, c \neq m$ | $p^{c=k}_{t+1} = \bar{P}_m - \mathrm{RU}^{a(k,m)}$<br>$p^c_t = 0, \forall c \in \mathcal{C}, c \neq m$ |
| $\lvert\mathcal{C}_{n\to}\rvert - 1$ | 0 | 0 | I | 0 | 0 | 0 | E | 0 | 0 | 0 | 0 | 0 | $p^{c=s}_{t+1} = \underline{P}_n + \mathrm{RU}^{a(n,s)}$<br>$p^c_{t+1} = 0, \forall c \in \mathcal{C}, c \neq s$ | $p^{c=n}_t = \underline{P}_n$<br>$p^c_t = 0, \forall c \in \mathcal{C}, c \neq n$ |
| $\sum_{k \in \mathcal{C}_{\to m}, k \neq n} (\lvert\mathcal{C}_{k\to}\rvert - 1)$ | 0 | 0 | 0 | I | 0 | 0 | 0 | 0 | E 0 0<br>0 ⋱ 0<br>0 0 E | 0 | 0 | 0 | $p^{c=k}_{t+1} = \underline{P}_k + \mathrm{RU}^{a(k,r)}$<br>$p^c_{t+1} = 0, \forall c \in \mathcal{C}, c \neq k$ | $p^{c=k}_t = \underline{P}_k$<br>$p^c_t = 0, \forall c \in \mathcal{C}, c \neq k$ |
| $\lvert\mathcal{C}\rvert - \lvert\mathcal{C}_{\to m}\rvert$ | 0 | 0 | 0 | 0 | I | 0 | 0 | 0 | 0 | 0 | I | 0 | $p^{c=x}_{t+1} = \underline{P}_x + \mathrm{RU}_{x,x}$<br>$p^c_{t+1} = 0, \forall c \in \mathcal{C}, c \neq x$ | $p^{c=x}_t = \underline{P}_x$<br>$p^c_t = 0, \forall c \in \mathcal{C}, c \neq x$ |
| $\lvert\mathcal{A}\rvert - \lvert\mathcal{C}\rvert + 1$<br>$- \sum_{k \in \mathcal{C}_{\to m}, k \neq n} (\lvert\mathcal{C}_{k\to} - 1\rvert)$<br>$- \lvert\mathcal{C}_{n\to}\rvert$ | 0 | 0 | 0 | 0 | 0 | I | 0 | 0 | 0 | 0 | E 0 0<br>0 ⋱ 0<br>0 0 E | 0 | $p^{c=y}_{t+1} = \underline{P}_x + \mathrm{RU}_{x,y}$<br>$p^c_{t+1} = 0, \forall c \in \mathcal{C}, c \neq y$ | $p^{c=x}_t = \underline{P}_x$<br>$p^c_t = 0, \forall c \in \mathcal{C}, c \neq x$ |
| 1 | 1 | 0 | 0 | 0 | 0 | 0 | 1 | 0 | 0 | 0 | 0 | 0 | $p^{c=m}_{t+1} = \underline{P}_n + \mathrm{RU}^{a(n,m)} + \epsilon$<br>$p^c_{t+1} = 0, \forall c \in \mathcal{C}, c \neq m$ | $p^{c=n}_t = \underline{P}_n + \epsilon$<br>$p^c_t = 0, \forall c \in \mathcal{C}, c \neq n$ |
| $\lvert\mathcal{C}_{\to n}\rvert - 1$ | E | 0 | 0 | 0 | 0 | 0 | 0 | I | 0 | 0 | 0 | 0 | $p^{c=m}_{t+1} = \underline{P}_n + \mathrm{RU}^{a(n,m)}$<br>$p^c_{t+1} = 0, \forall c \in \mathcal{C}, c \neq m$ | $p^{c=n}_t = \underline{P}_n$<br>$p^c_t = 0, \forall c \in \mathcal{C}, c \neq n$ |
| $\lvert\mathcal{C}_{\to m}\rvert - 1$ | 0 | I | 0 | 0 | 0 | 0 | 0 | 0 | I | 0 | 0 | 0 | $p^{c=m}_{t+1} = \bar{P}_m$<br>$p^c_{t+1} = 0, \forall c \in \mathcal{C}, c \neq m$ | $p^{c=k}_{t+1} = \bar{P}_m - \mathrm{RU}^{a(k,m)} + \epsilon$<br>$p^c_t = 0, \forall c \in \mathcal{C}, c \neq k$ |
| $\sum_{k \in \mathcal{C}_{\to m}, k \neq n} (\lvert\mathcal{C}_{\to k}\rvert - 1)$ | 0 | E 0 0<br>0 ⋱ 0<br>0 0 E | 0 | 0 | 0 | 0 | 0 | 0 | 0 | I | 0 | 0 | $p^{c=m}_{t+1} = \bar{P}_m$<br>$p^c_{t+1} = 0, \forall c \in \mathcal{C}, c \neq m$ | $p^{c=k}_{t+1} = \bar{P}_m - \mathrm{RU}^{a(k,m)}$<br>$p^c_t = 0, \forall c \in \mathcal{C}, c \neq k$ |
| $\lvert\mathcal{C}\rvert - \lvert\mathcal{C}_{\to m}\rvert$ | 0 | 0 | 0 | 0 | I | 0 | 0 | 0 | 0 | 0 | I | 0 | $p^{c=x}_{t+1} = \underline{P}_x + \mathrm{RU}^{a(x,x)} + \epsilon$<br>$p^c_{t+1} = 0, \forall c \in \mathcal{C}, c \neq x$ | $p^{c=x}_t = \underline{P}_x + \epsilon$<br>$p^c_t = 0, \forall c \in \mathcal{C}, c \neq x$ |
| $\lvert\mathcal{A}\rvert - \lvert\mathcal{C}\rvert + 1$<br>$- \sum_{k \in \mathcal{C}_{\to m}, k \neq n} (\lvert\mathcal{C}_{\to k}\rvert)$<br>$- \lvert\mathcal{C}_{\to n}\rvert$ | 0 | 0 | 0 | 0 | E 0 0<br>0 ⋱ 0<br>0 0 E | 0 | 0 | 0 | 0 | 0 | 0 | I | $p^{c=x}_{t+1} = \underline{P}_x + \mathrm{RU}^{a(x,x)}$<br>$p^c_{t+1} = 0, \forall c \in \mathcal{C}, c \neq x$ | $p^{c=x}_t = \underline{P}_x$<br>$p^c_t = 0, \forall c \in \mathcal{C}, c \neq x$ |
| $\lvert\mathcal{C}\rvert - \lvert\mathcal{C}_{\to m}\rvert$ | 0 | 0 | 0 | 0 | I | 0 | 0 | 0 | 0 | 0 | 0 | $E_1$ 0 ⋯ 0 0<br>0 $E_1$ ⋯ 0 0<br>0 0 ⋱ 0 0<br>0 0 ⋯ $E_1$ 0<br>0 0 ⋯ 0 $E_1$ | $p^{c=x}_{t+1} = \underline{P}_x + \mathrm{RU}^{a(x,x)} + \epsilon$<br>$p^c_{t+1} = 0, \forall c \in \mathcal{C}, c \neq x$ | $p^{c=x}_t = \underline{P}_x + \epsilon$<br>$p^c_t = 0, \forall c \in \mathcal{C}, c \neq x$ |
| $\lvert\mathcal{C}_{\to m}\rvert - 1$ | 0 | I | 0 | 0 | 0 | 0 | 0 | 0 | 0 | $E_1$ 0 ⋯ 0 0<br>0 $E_1$ ⋯ 0 0<br>0 0 ⋱ 0 0<br>0 0 ⋯ $E_1$ 0<br>0 0 ⋯ 0 $E_1$ | 0 | 0 | $p^{c=m}_{t+1} = \bar{P}_m$<br>$p^c_{t+1} = 0, \forall c \in \mathcal{C}, c \neq m$ | $p^{c=k}_t = \bar{P}_m - \mathrm{RU}^{a(k,m)} + \epsilon$<br>$p^c_t = 0, \forall c \in \mathcal{C}, c \neq k$ |

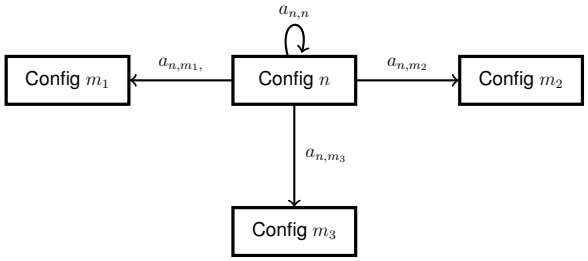


Fig. 4. Configuration Transition Graph for Configuration $n$

up/down inequalities can be described as follows:

$$p_{t+1}^m - \sum_{n\in\mathcal{C}_{\to m}} p_t^n \le \sum_{n\in\mathcal{C}_{\to m}} \text{RU}^{a(n,m)} z_{t+1}^{a(n,m)} \tag{47}$$
$$- \sum_{n\in\mathcal{C}_{\to m}} \underline{P}_n \Big( \Big( \sum_{a\in(\mathcal{A}_n^{\text{in}} \bigcup \mathcal{A}_n^{\text{sl}})} z_t^a \Big) - z_{t+1}^{a(n,m)} \Big), \forall m \in \mathcal{C}, \forall t,$$

$$\sum_{n\in\mathcal{C}_{\to m}} p_t^n - p_{t+1}^m \le \sum_{n\in\mathcal{C}_{\to m}} \text{RD}^{a(n,m)} z_{t+1}^{a(n,m)} \tag{48}$$
$$+ \sum_{n\in\mathcal{C}_{\to m}} \bar{P}_n \Big( \Big( \sum_{a\in(\mathcal{A}_n^{\text{in}} \bigcup \mathcal{A}_n^{\text{sl}})} z_t^a \Big) - z_{t+1}^{a(n,m)} \Big), \forall m \in \mathcal{C}, \forall t.$$

In inequalities (47) and (48), $\mathcal{C}_{\to m}$ represents the set of configurations which can transition to Configuration $m$. For example, in Fig. 3, $\mathcal{C}_{\to m} = \{n_1, n_2, n_3\}$. First, we show the validity of ramping up inequalities (47) by discussing three possible cases as follows:

Case 1: the combined-cycle unit works on Configuration $m$ at time period $t+1$. In this case one of the incoming arcs or the self-loop arc of Configuration $m$ is active at time period $t+1$. For instance, in Fig. 3, one of the arcs $\{a_{n_1,m}, a_{n_2,m}, a_{n_3,m}, a_{m,m}\}$ is active at time period $t+1$. Suppose that the combined-cycle unit works on Configuration $\bar{n}$ at time period $t$, where $\bar{n} \in \mathcal{C}_{\to m}$. Consequently, arc $a(\bar{n}, m)$ is active at time period $t+1$. In this case, we have $z_{t+1}^{a(\bar{n},m)} = 1$, $z_{t+1}^{a(\hat{n},m)} = 0$, $\sum_{a\in(\mathcal{A}_{\bar{n}}^{\text{in}} \bigcup \mathcal{A}_{\bar{n}}^{\text{sl}})} z_t^a = 1$, and $\sum_{a\in(\mathcal{A}_{\hat{n}}^{\text{in}} \bigcup \mathcal{A}_{\hat{n}}^{\text{sl}})} z_t^a = 0$, where $\hat{n} \in \mathcal{C}_{\to m} \setminus \{\bar{n}\}$. It follows that inequalities (47) convert to $p_{t+1}^m - p_t^{\bar{n}} \le \text{RU}^{a(\bar{n},m)}$, which is valid due to constraints (17).

Case 2: the combined-cycle unit does not work on Configuration $m$ at time period $t+1$. However, the combined-cycle unit works on Configuration $\bar{n}$ at time period $t$, where $\bar{n} \in \mathcal{C}_{\to m}$. In this case, all of the incoming arcs and the self-loop arc of Configuration $m$ are not active at time period $t+1$, which means $z_{t+1}^{a(n,m)} = 0, \forall n \in \mathcal{C}_{\to m}$. In addition, we have $\sum_{a\in(\mathcal{A}_{\bar{n}}^{\text{in}} \bigcup \mathcal{A}_{\bar{n}}^{\text{sl}})} z_t^a = 1$ and $\sum_{a\in(\mathcal{A}_{\hat{n}}^{\text{in}} \bigcup \mathcal{A}_{\hat{n}}^{\text{sl}})} z_t^a = 0$, where $\hat{n} \in \mathcal{C}_{\to m} \setminus \{\bar{n}\}$. Then, inequalities (47) reduce to $-p_t^{\bar{n}} \le -\underline{P}_{\bar{n}}$, which is valid because of constraints (12).

Case 3: the combined-cycle unit does not work on Configuration $m$ at time period $t+1$. Meanwhile, it does not work on any configuration in set $\mathcal{C}_{\to m}$ at time period $t$. In this case, all decision variables become zero in inequalities (47). Both the left and right sides of (47) will be equal to zero.

We summarize this analysis in Table V. Furthermore, we list the analogous analysis for (48) in Table VI. In these two tables, $\sum_{n\in\mathcal{C}_{\to m}} z_{t+1}^{a(n,m)}$ indicates whether Configuration $m$ is online at time period $t+1$. In addition, $\sum_{n\in\mathcal{C}_{\to m}} \sum_{a\in(\mathcal{A}_n^{\text{in}} \bigcup \mathcal{A}_n^{\text{sl}})} z_t^a$ indicates whether any configuration in $\mathcal{C}_{\to m}$ is online. We specifically let $\bar{n}$ represent the online configuration in $\mathcal{C}_{\to m}$.

TABLE V
VALIDITY OF RAMPING UP INEQUALITIES (47)

| Case | Value of Binary Variables | | Inequality | |
|---|---|---|---|---|
| | $\sum_{n\in\mathcal{C}_{\to m}} z_{t+1}^{a(n,m)}$ | $\sum_{n\in\mathcal{C}_{\to m}} \sum_{a\in(\mathcal{A}_n^{\text{in}} \bigcup \mathcal{A}_n^{\text{sl}})} z_t^a$ | LHS | RHS |
| 1 | 1 | 1 | $p_{t+1}^m - p_t^{\bar{n}}$ | $\text{RU}^{a(\bar{n},m)}$ |
| 2 | 0 | 1 | $-p_t^{\bar{n}}$ | $-\underline{P}_{\bar{n}}$ |
| 3 | 0 | 0 | 0 | 0 |

TABLE VI
VALIDITY OF RAMPING DOWN INEQUALITIES (48)

| Case | Value of Binary Variables | | Inequality | |
|---|---|---|---|---|
| | $\sum_{n\in\mathcal{C}_{\to m}} z_{t+1}^{a(n,m)}$ | $\sum_{n\in\mathcal{C}_{\to m}} \sum_{a\in(\mathcal{A}_n^{\text{in}} \bigcup \mathcal{A}_n^{\text{sl}})} z_t^a$ | LHS | RHS |
| 1 | 1 | 1 | $p_t^{\bar{n}} - p_{t+1}^m$ | $\text{RD}^{a(\bar{n},m)}$ |
| 2 | 0 | 1 | $p_t^{\bar{n}}$ | $\bar{P}_{\bar{n}}$ |
| 3 | 0 | 0 | 0 | 0 |

Next, for each $m \in \mathcal{C}$ and $t$, we show inequality (47) is facet-defining for the projection of the whole feasible space (denoted as $\mathcal{Q}$) onto $\mathcal{S} = \{z_t^a, z_{t+1}^a, p_t^n, p_{t+1}^n, \ \forall a \in \mathcal{A}, \forall n \in \mathcal{C}\}$ when $\underline{P}_m \le \underline{P}_n + \text{RU}^{a(n,m)} < \bar{P}_m, \ \forall n \in \mathcal{C}_{\to m}$, where $\mathcal{S}$ consists of all the variables describing inequality (47). As there are $2(|\mathcal{A}| + |\mathcal{C}|)$ variables in $\mathcal{S}$, $\sum_{a\in(\mathcal{A}_k^{\text{in}} \bigcup \mathcal{A}_k^{\text{sl}})} z_t^a = \sum_{a\in(\mathcal{A}_k^{\text{out}} \bigcup \mathcal{A}_k^{\text{sl}})} z_{t+1}^a, \forall k \in \mathcal{C}$, and $\sum_{a\in\mathcal{A}} z_t^a = 1$, the dimension of the projection of $\mathcal{Q}$ onto $\mathcal{S}$ is $2|\mathcal{A}| + |\mathcal{C}| - 1$. In the following, we provide $2|\mathcal{A}| + |\mathcal{C}| - 1$ affinely independent points that satisfy (47) at equality to show the property of facet-defining [21], see Table VII.

In Table VII, there are 11 groups of points in total, with each row representing one point satisfying (47) at equality and each column representing the value of each variable. Meanwhile, we let $I$ represent an identity matrix and 0 represent a zero matrix. We generate these points in the following ways:

1) In Groups 1 - 3, we construct a lower matrix in terms of the value of $z_t^a, \ \forall a \in \mathcal{A}$. In particular, in Group 1, for each $k \in \mathcal{C}_{\to m}$ (totally $|\mathcal{C}_{\to m}|$ points), we let $z_t^{a(k,m)} = 1$, $z_{t+1}^{a(m,m)} = 1$, $p_t^m = \underline{P}_m$, and $p_{t+1}^m = \underline{P}_m + \text{RU}^{a(m,m)}$; in Group 2, for each $s \in \mathcal{C}_{m\to}, \ s \ne m$ (totally $|\mathcal{C}_{m\to}| - 1$ points, note that we rule out $s = m$ to avoid duplication), we let $z_t^{a(m,s)} = 1$, $z_{t+1}^{a(s,s)} = 1$, and $p_t^s = p_{t+1}^s = \underline{P}_s$; in Group 3, for each remaining arcs of $\mathcal{A}$ (totally $|\mathcal{A}| - |\mathcal{C}_{\to m}| - (|\mathcal{C}_{m\to}| - 1)$ points), i.e., $(x, y)$, we let $z_t^{a(x,y)} = 1$, $z_{t+1}^{a(y,y)} = 1$, $p_t^y = \underline{P}_y$, and $p_{t+1}^y = \underline{P}_y$. Therefore, in total we generate $|\mathcal{A}|$ points here.
2) In Groups 4 - 6, we continue to construct a lower matrix in terms of the value of $z_{t+1}^a, \ \forall a \in \mathcal{A}$, which together with the lower matrix generated in Groups 1 - 3 can be easily transformed to a large lower matrix through Gaussian elimination. In particular, in Group 4, for each $k \in \mathcal{C}_{\to m}, \ k \ne m$ (totally $|\mathcal{C}_{\to m}| - 1$ points, note that we rule out $k = m$ to avoid duplicating one point in group 1), we let $z_t^{a(k,k)} = 1$, $z_{t+1}^{a(k,m)} = 1$, $p_t^k = \underline{P}_k$, and $p_{t+1}^m = \underline{P}_k + \text{RU}^{a(k,m)}$; in Group 5, for each

$s \in \mathcal{C}_{m\rightarrow},\ s \neq m$ (totally $|\mathcal{C}_{m\rightarrow}|-1$ points), we let $z_t^{a(m,m)}=1$, $z_{t+1}^{a(m,s)}=1$, $p_t^m=\underline{P}_m$, and $p_{t+1}^s=\underline{P}_s$; in Group 6, for each remaining arcs of $\mathcal{A}\setminus\{(n,n),\forall n\in\mathcal{C}\}$ (totally $|\mathcal{A}|-|\mathcal{C}|-(|\mathcal{C}_{\rightarrow m}|-1)-(|\mathcal{C}_{m\rightarrow}|-1)$ points, note that we rule out $(n,n),\forall n\in\mathcal{C}$ to avoid duplication with Groups 1 - 3), i.e., $(x,y)$ with $x\neq y$, we let $z_t^{a(x,x)}=1$, $z_{t+1}^{a(x,y)}=1$, $p_t^x=\underline{P}_x$, and $p_{t+1}^y=\underline{P}_y$. Therefore, in total we generate $|\mathcal{A}|-|\mathcal{C}|$ points here.

3) In Groups 7 - 9, we generate $|\mathcal{C}|$ points by utilizing the points in Groups 1 - 3 so that the points in these groups together with the points above can be easily transformed to a lower matrix. In particular, in Group 7 (totally one point), we choose one $\bar{k}\in\mathcal{C}_{\rightarrow m}$ (e.g., $\bar{k}=m$) and let $z_t^{a(\bar{k},m)}=1$, $z_{t+1}^{a(m,m)}=1$, $p_t^m=\underline{P}_m+\epsilon$, and $p_{t+1}^m=\underline{P}_m+\text{RU}^{a(m,m)}+\epsilon$; in Group 8, for each $s\in\mathcal{C}_{m\rightarrow},\ s\neq m$ (totally $|\mathcal{C}_{m\rightarrow}|-1$ points), we let $z_t^{a(m,s)}=1$, $z_{t+1}^{a(s,s)}=1$, and $p_t^s=p_{t+1}^s=\underline{P}_s+\epsilon$; in Group 9, for each remaining configuration of $\mathcal{C}$ (totally $|\mathcal{C}|-1-(|\mathcal{C}_{m\rightarrow}|-1)$ points), i.e., $(x,y)$ with $y\in\mathcal{C}\setminus\{\mathcal{C}_{m\rightarrow}\}$ for some $x$, we let $z_t^{a(x,y)}=1$, $z_{t+1}^{a(y,y)}=1$, $p_t^y=\underline{P}_y+\epsilon$, and $p_{t+1}^y=\underline{P}_y+\epsilon$. Therefore, in total we generate $|\mathcal{C}|$ points here. We can easily observe that the points in Groups 7-9 together with the points in Groups 1-3 can be transformed to a lower matrix in terms of the values of $z_t^a,\ \forall a\in\mathcal{A}$ and $p_{t+1}^n,\ \forall n\in\mathcal{C}$.

4) In Groups 10 - 11, we generate $|\mathcal{C}|-1$ points by utilizing the points in Groups 4 - 6 so that the points in these groups together with the points above can be easily transformed to a lower matrix. In particular, in Group 10, for each $k\in\mathcal{C}_{\rightarrow m},\ k\neq m$ (totally $|\mathcal{C}_{\rightarrow m}|-1$ points), we let $z_t^{a(k,k)}=1$, $z_{t+1}^{a(k,m)}=1$, $p_t^k=\underline{P}_k+\epsilon$, and $p_{t+1}^m=\underline{P}_k+\text{RU}^{a(k,m)}+\epsilon$; in Group 11, for each remaining configuration of $\mathcal{C}\setminus\mathcal{C}_{\rightarrow m}$ (totally $|\mathcal{C}|-(|\mathcal{C}_{\rightarrow m}|-1)-1$ points), i.e., $(x,y)$ with $x\in\mathcal{C}\setminus\mathcal{C}_{\rightarrow m}$ for some $y$ and $x\in\{m,y\}$, we let $z_t^{a(x,x)}=1$, $z_{t+1}^{a(x,y)}=1$, $p_t^x=\underline{P}_x+\epsilon$, and $p_{t+1}^y=\underline{P}_y+\epsilon$. Thus, in total we generate $|\mathcal{C}|-1$ points here. We can easily observe that the points in Groups 10-11 together with the points in Groups 4-6 can be transformed to a lower matrix in terms of the values of $z_{t+1}^a,\ \forall a\in\mathcal{A}$ and $p_t^n,\ \forall n\in\mathcal{C}\setminus\{m\}$.

In summary, it is clear that $2|\mathcal{A}|+|\mathcal{C}|-1$ points generated above satisfy (47) at equality and can easily be transformed to a lower matrix with dimension at least $2|\mathcal{A}|+|\mathcal{C}|-2$, which means that these points are affinely independent.

Inequalities (48) and the following inequalities (49) and (50) can be similarly shown to be facet-defining under mild conditions and thus we omit the corresponding facet-defining proofs due to page limit and only provide the validity proofs.

For the scenario captured in Fig. 4, we develop ramping up/down inequalities (49) and (50). In these inequalities, $\mathcal{C}_{n\rightarrow}$ represents the set of configurations to which Configuration $n$ can transition. For instance, in Fig. 4, $\mathcal{C}_{n\rightarrow}=\{m_1,m_2,m_3\}$. In order to verify the validity of inequalities (49), we analyze three possible cases. A similar procedure can be applied to verify the validity of inequalities (50).

$$\sum_{m\in\mathcal{C}_{n\rightarrow}} p_{t+1}^m-p_t^n\leq\sum_{m\in\mathcal{C}_{n\rightarrow}}\text{RU}^{a(n,m)}z_{t+1}^{a(n,m)} \tag{49}$$

$$+\sum_{m\in\mathcal{C}_{n\rightarrow}}\bar{P}_m\Big(\Big(\sum_{a\in(\mathcal{A}_m^{\text{in}}\bigcup\mathcal{A}_m^{\text{sl}})}z_{t+1}^a\Big)-z_{t+1}^{a(n,m)}\Big),\forall n\in\mathcal{C},\forall t,$$

$$p_n^t-\sum_{m\in\mathcal{C}_{n\rightarrow}}p_{t+1}^m\leq\sum_{m\in\mathcal{C}_{n\rightarrow}}\text{RD}^{a(n,m)}z_{t+1}^{a(n,m)} \tag{50}$$

$$-\sum_{m\in\mathcal{C}_{n\rightarrow}}\underline{P}_m\Big(\Big(\sum_{a\in(\mathcal{A}_m^{\text{in}}\bigcup\mathcal{A}_m^{\text{sl}})}z_{t+1}^a\Big)-z_{t+1}^{a(n,m)}\Big),\forall n\in\mathcal{C},\forall t.$$

Case 1: the combined-cycle unit works on Configuration $n$ at time period $t$ and on one of the configurations (denoted as $\bar{m}$) in $\mathcal{C}_{n\rightarrow}$ at time period $t+1$. In this case, we have $z_{t+1}^{a(n,\bar{m})}=1, z_{t+1}^{a(n,\hat{m})}=0, \sum_{a\in(\mathcal{A}_{\bar{m}}^{\text{in}}\bigcup\mathcal{A}_{\bar{m}}^{\text{sl}})}z_{t+1}^a=1$, and $\sum_{a\in(\mathcal{A}_{\hat{m}}^{\text{in}}\bigcup\mathcal{A}_{\hat{m}}^{\text{sl}})}z_{t+1}^a=0$, where $\hat{m}\in\mathcal{C}_{n\rightarrow}\setminus\{\bar{m}\}$. Then inequalities (49) convert to $p_{t+1}^{\bar{m}}-p_t^n\leq\text{RU}^{a(n,\bar{m})}$ which is valid due to constraints (17).

Case 2: the combined-cycle unit does not work on Configuration $n$ at time period $t$. However, it works on one of the configurations (denoted as $\bar{m}$) in $\mathcal{C}_{n\rightarrow}$ at time period $t+1$. In this case, we have $z_{t+1}^{a(n,\bar{m})}=0, z_{t+1}^{a(n,\hat{m})}=0, \sum_{a\in(\mathcal{A}_{\bar{m}}^{\text{in}}\bigcup\mathcal{A}_{\bar{m}}^{\text{sl}})}z_{t+1}^a=1$, and $\sum_{a\in(\mathcal{A}_{\hat{m}}^{\text{in}}\bigcup\mathcal{A}_{\hat{m}}^{\text{sl}})}z_{t+1}^a=0$, where $\hat{m}\in\mathcal{C}_{n\rightarrow}\setminus\{\bar{m}\}$. Then inequalities (49) convert to $p_{t+1}^{\bar{m}}\leq\bar{P}_{\bar{m}}$, which is valid due to constraints (13).

Case 3: the combined-cycle unit neither works on Configuration $n$ at time period $t$, nor works on any configuration in $\mathcal{C}_{n\rightarrow}$ at time period $t+1$. In this case, all decision variables in inequalities (49) take zeros.

TABLE VIII
VALIDITY OF RAMPING UP INEQUALITIES (49)

| Case | Value of Binary Variables | | Inequality | |
|---|---|---|---|---|
| | $\sum_{m\in\mathcal{C}_{n\rightarrow}}z_{t+1}^{a(n,m)}$ | $\sum_{m\in\mathcal{C}_{n\rightarrow}}\sum_{a\in(\mathcal{A}_m^{\text{in}}\bigcup\mathcal{A}_m^{\text{sl}})}z_{t+1}^a$ | LHS | RHS |
| 1 | 1 | 1 | $p_{t+1}^{\bar{m}}-p_t^n$ | $\text{RU}^{a(n,\bar{m})}$ |
| 2 | 0 | 1 | $p_t^{\bar{m}}$ | $\bar{P}_{\bar{m}}$ |
| 3 | 0 | 0 | 0 | 0 |

TABLE IX
VALIDITY OF RAMPING DOWN INEQUALITIES (50)

| Case | Value of Binary Variables | | Inequality | |
|---|---|---|---|---|
| | $\sum_{m\in\mathcal{C}_{n\rightarrow}}z_{t+1}^{a(n,m)}$ | $\sum_{m\in\mathcal{C}_{n\rightarrow}}\sum_{a\in(\mathcal{A}_m^{\text{in}}\bigcup\mathcal{A}_m^{\text{sl}})}z_{t+1}^a$ | LHS | RHS |
| 1 | 1 | 1 | $p_t^n-p_{t+1}^{\bar{m}}$ | $\text{RD}^{a(n,\bar{m})}$ |
| 2 | 0 | 1 | $-p_t^{\bar{m}}$ | $-\underline{P}_{\bar{m}}$ |
| 3 | 0 | 0 | 0 | 0 |

Tables VIII and IX show the validity analysis of ramping rate inequalities (49) and (50), respectively. In the second row of these tables, item $\sum_{m\in\mathcal{C}_{n\rightarrow}}z_{t+1}^{a(n,m)}$ represents the status of Configuration $n$ at time period $t$. In addition, if $\sum_{m\in\mathcal{C}_{n\rightarrow}}\sum_{a\in(\mathcal{A}_m^{\text{in}}\bigcup\mathcal{A}_m^{\text{sl}})}z_{t+1}^a=1$, then one of the configurations in $\mathcal{C}_{n\rightarrow}$ is online at time period $t+1$. We specifically let $\bar{m}$ represent this online configuration. Otherwise, all configurations in $\mathcal{C}_{n\rightarrow}$ are offline at time period $t+1$.

## V. COMPUTATIONAL RESULTS

In this section, we test the performance of our strengthened edge-based formulation (SEBF) on a modified IEEE 118-bus power system [22] by solving a unit commitment (UC) problem with combined-cycle units. The objective is to minimize

TABLE VII
$2|\mathcal{A}| + |\mathcal{C}| - 1$ AFFINELY INDEPENDENT POINTS FOR (47)

| # Point | $z_t^a,\ \forall a \in \mathcal{A}$ | | | $z_{t+1}^a,\ \forall a \in \mathcal{A}$ | | | $p_t^n,\ \forall n \in \mathcal{C}$ | | | | | $p_{t+1}^n,\ \forall n \in \mathcal{C}$ | | | | |
|---|---|---|---|---|---|---|---|---|---|---|---|---|---|---|---|---|
| | $(k,m), \forall k \in \mathcal{C}_{\to m}$ | $(m,s), \forall s \in \mathcal{C}_{m\to}$ $s \neq m$ | $(x,y)$ $x \neq m$ $y \neq m$ | $(k,m), \forall k \in \mathcal{C}_{\to m}$ | $(m,s), \forall s \in \mathcal{C}_{m\to}$ $s \neq m$ | $(x,y)$ $x \neq m$ $y \neq m$ | $\forall k \in \mathcal{C}_{\to m}$ | $m$ | $(m,s), \forall s \in \mathcal{C}_{m\to}$ $s \neq m$ | $x \neq m$ | $y \neq m$ | $\forall k \in \mathcal{C}_{\to m}$ | $m$ | $(m,s), \forall s \in \mathcal{C}_{m\to}$ $s \neq m$ | $x \neq m$ | $y \neq m$ |
| $\lvert\mathcal{C}_{\to m}\rvert$ | I | 0 | 0 | $z_{t+1}^{a(k,m)} = 1$, if $k = m$; 0, $o.w.$ | 0 | 0 | 0 | $\underline{P}_m$<br>$\underline{P}_m$<br>$\underline{P}_m$ | 0 | 0 | 0 | 0 | $\underline{P}_m + \underline{\mathrm{RU}}^{a(m,m)}$<br>$\underline{P}_m + \underline{\mathrm{RU}}^{a(m,m)}$<br>$\underline{P}_m + \underline{\mathrm{RU}}^{a(m,m)}$ | 0 | 0 | 0 |
| $\lvert\mathcal{C}_{m\to}\rvert - 1$ | 0 | I | 0 | 0 | 0 | $z_{t+1}^{a(s,s)} = 1$ | 0 | 0<br>0<br>0 | $\underline{P}_s$ 0<br>$\cdots$<br>0 $\underline{P}_s$ | 0 | 0 | 0 | 0<br>0<br>0 | $\underline{P}_s$ 0<br>$\cdots$<br>0 $\underline{P}_s$ | 0 | 0 |
| $\lvert\mathcal{A}\rvert + 1 - \lvert\mathcal{C}_{\to m}\rvert - \lvert\mathcal{C}_{m\to}\rvert$ | 0 | 0 | I | 0 | 0 | $z_{t+1}^{a(y,y)} = 1$ | 0 | 0<br>0<br>0 | 0 | 0 | $\underline{P}_y$ 0<br>$\cdots$<br>0 $\underline{P}_y$ | 0 | 0<br>0<br>0 | 0 | 0 | $\underline{P}_y$ 0<br>$\cdots$<br>0 $\underline{P}_y$ |
| $\lvert\mathcal{C}_{\to m}\rvert - 1$ | 0 | 0 | $z_t^{a(k,k)} = 1$ | I<br>$(k \neq m)$ | 0 | 0 | $\underline{P}_k$ 0<br>$\cdots$<br>0 $\underline{P}_k$ | 0<br>0<br>0 | 0 | 0 | 0 | 0 | $\underline{P}_k + \underline{\mathrm{RU}}^{a(k,m)}$<br>$\underline{P}_k + \underline{\mathrm{RU}}^{a(k,m)}$<br>$\underline{P}_k + \underline{\mathrm{RU}}^{a(k,m)}$ | 0 | 0 | 0 |
| $\lvert\mathcal{C}_{m\to}\rvert - 1$ | $z_t^{a(m,m)} = 1$ | 0 | 0 | 0 | I | 0 | 0 | $\underline{P}_m$<br>$\underline{P}_m$<br>$\underline{P}_m$ | 0 | 0 | 0 | 0 | 0<br>0<br>0 | $\underline{P}_s$ 0<br>$\cdots$<br>0 $\underline{P}_s$ | 0 | 0 |
| $\lvert\mathcal{A}\rvert - \lvert\mathcal{C}\rvert + 2 - \lvert\mathcal{C}_{\to m}\rvert - \lvert\mathcal{C}_{m\to}\rvert$ | 0 | 0 | $z_t^{a(x,x)} = 1$ $x \neq y$ | 0 | 0 | I | 0 | 0<br>0<br>0 | 0 | $\underline{P}_x$ 0<br>$\cdots$<br>0 $\underline{P}_x$ | 0 | 0 | 0<br>0<br>0 | 0 | 0 | $\underline{P}_y$ 0<br>$\cdots$<br>0 $\underline{P}_y$ |
| 1 | 1 0 0 | 0 0 0 | 0 0 0 | 0 0 1 | 0 0 0 | 0 0 0 | 0 0 | $\underline{P}_m + \epsilon$ | 0 0 | 0 0 | 0 0 | 0 0 | $\underline{P}_m + \epsilon + \underline{\mathrm{RU}}^{a(m,m)}$ | 0 0 | 0 0 | 0 0 |
| $\lvert\mathcal{C}_{m\to}\rvert - 1$ | 0 | I | 0 | 0 | 0 | $z_{t+1}^{a(s,s)} = 1$ | 0 | 0<br>0<br>0 | $\underline{P}_s + \epsilon$ 0<br>$\cdots$<br>0 $\underline{P}_s + \epsilon$ | 0 | 0 | 0 | 0<br>0<br>0 | $\underline{P}_s + \epsilon$ 0<br>$\cdots$<br>0 $\underline{P}_s + \epsilon$ | 0 | 0 |
| $\lvert\mathcal{C}\rvert - \lvert\mathcal{C}_{m\to}\rvert$ | 0 | 0 | I | 0 | 0 | $z_{t+1}^{a(y,y)} = 1$ | 0 | 0<br>0<br>0 | 0 | 0 | $\underline{P}_y + \epsilon$ 0<br>$\cdots$<br>0 $\underline{P}_y + \epsilon$ | 0 | 0<br>0<br>0 | 0 | 0 | $\underline{P}_y + \epsilon$ 0<br>$\cdots$<br>0 $\underline{P}_y + \epsilon$ |
| $\lvert\mathcal{C}_{\to m}\rvert - 1$ | 0 | 0 | $z_t^{a(k,k)} = 1$ | I<br>$(k \neq m)$ | 0 | 0 | $\underline{P}_k + \epsilon$ 0<br>$\cdots$<br>0 $\underline{P}_k + \epsilon$ | 0<br>0<br>0 | 0 | 0 | 0 | 0 | $\underline{P}_k + \epsilon + \underline{\mathrm{RU}}^{a(k,m)}$<br>$\underline{P}_k + \epsilon + \underline{\mathrm{RU}}^{a(k,m)}$<br>$\underline{P}_k + \epsilon + \underline{\mathrm{RU}}^{a(k,m)}$ | 0 | 0 | 0 |
| $\lvert\mathcal{C}\rvert - \lvert\mathcal{C}_{\to m}\rvert$ | 0 | 0 | $z_t^{a(x,x)} = 1$ $x \neq y$ | 0 | 0 | I | 0 | 0<br>0<br>0 | 0 | $\underline{P}_x + \epsilon$ 0<br>$\cdots$<br>0 $\underline{P}_x + \epsilon$ | 0 | 0 | 0<br>0<br>0 | 0 | 0 | $\underline{P}_y + \epsilon$ 0<br>$\cdots$<br>0 $\underline{P}_y + \epsilon$ |

TABLE X
ROOT NODE INFORMATION

| Case | | MIP Objective Values ($) | | | | LP Objective Values ($) | | | | Integrality Gap ($10^{-4}$) | | | |
|---|---|---|---|---|---|---|---|---|---|---|---|---|---|
| | | EBF | TEBF | REBF | SEBF | EBF | TEBF | REBF | SEBF | EBF | TEBF | REBF | SEBF |
| One-day | 1 | 1881741 | 1881738 | 1881740 | 1881741 | 1879876 | 1880212 | 1880451 | 1880774 | 9.92 | 8.11 | 6.85 | 5.14 |
| | 2 | 1881012 | 1881017 | 1881032 | 1881034 | 1879103 | 1879456 | 1879698 | 1880031 | 10.15 | 8.30 | 7.10 | 5.34 |
| | 3 | 1887049 | 1887052 | 1887046 | 1887049 | 1885160 | 1885489 | 1885739 | 1886056 | 10.01 | 8.29 | 6.93 | 5.26 |
| | 4 | 1878048 | 1878051 | 1878045 | 1878036 | 1876169 | 1876512 | 1876746 | 1877070 | 10.01 | 8.19 | 6.96 | 5.15 |
| | 5 | 1888911 | 1888950 | 1888948 | 1888927 | 1887136 | 1887470 | 1887715 | 1888032 | 9.39 | 7.84 | 6.53 | 4.74 |
| | 6 | 1882816 | 1882810 | 1882829 | 1882829 | 1881003 | 1881349 | 1881587 | 1881917 | 9.63 | 7.76 | 6.60 | 4.85 |
| | 7 | 1885035 | 1885046 | 1885037 | 1885032 | 1883170 | 1883519 | 1883780 | 1884109 | 9.89 | 8.09 | 6.67 | 4.90 |
| | 8 | 1894861 | 1894858 | 1894877 | 1894871 | 1893035 | 1893377 | 1893613 | 1893933 | 9.63 | 7.82 | 6.67 | 4.95 |
| | 9 | 1882781 | 1882797 | 1882765 | 1882792 | 1880881 | 1881227 | 1881447 | 1881777 | 10.09 | 8.34 | 6.99 | 5.39 |
| | 10 | 1889614 | 1889610 | 1889603 | 1889614 | 1887748 | 1888090 | 1888332 | 1888656 | 9.88 | 8.05 | 6.73 | 5.07 |
| Two-day | 1 | 3618451 | 3618497 | 3618534 | 3618859 | 3615129 | 3615571 | 3616036 | 3616440 | 9.18 | 8.08 | 6.90 | 6.68 |
| | 2 | 3610532 | 3610156 | 3610275 | 3610458 | 3606929 | 3607372 | 3607865 | 3608274 | 9.98 | 7.72 | 6.68 | 6.05 |
| | 3 | 3606894 | 3606396 | 3606304 | 3606337 | 3602757 | 3603224 | 3603670 | 3604094 | 11.47 | 8.79 | 7.30 | 6.2 |
| | 4 | 3612798 | 3612972 | 3612785 | 3613001 | 3609224 | 3609688 | 3610134 | 3610562 | 9.89 | 9.09 | 7.34 | 6.75 |
| | 5 | 3611288 | 3610916 | 3610919 | 3610702 | 3607151 | 3607576 | 3608070 | 3608472 | 11.45 | 9.25 | 7.89 | 6.17 |
| | 6 | 3615004 | 3614481 | 3614156 | 3614315 | 3611081 | 3611530 | 3611981 | 3612397 | 10.85 | 8.16 | 6.02 | 5.30 |
| | 7 | 3608393 | 3608558 | 3608302 | 3608537 | 3605084 | 3605514 | 3605995 | 3606396 | 9.16 | 8.43 | 6.39 | 5.93 |
| | 8 | 3603924 | 3603867 | 3604570 | 3604011 | 3600694 | 3601132 | 3601625 | 3602030 | 8.96 | 7.58 | 8.17 | 5.49 |
| | 9 | 3609562 | 3608981 | 3609269 | 3609336 | 3605444 | 3605881 | 3606415 | 3606817 | 11.41 | 8.59 | 7.90 | 6.97 |
| | 10 | 3604755 | 3605234 | 3605078 | 3605172 | 3601242 | 3601700 | 3602198 | 3602625 | 9.75 | 9.80 | 7.98 | 7.06 |

TABLE XI
COMPUTATIONAL TIMES

| case | | Time | | | | Number of Nodes | | | |
|---|---|---|---|---|---|---|---|---|---|
| | | EBF | TEBF | REBF | SEBF | EBF | TEBF | REBF | SEBF |
| One-day | 1 | 1668.92 | 1478.32 | 1208.08 | 650.23 | 4526 | 3315 | 2537 | 1064 |
| | 2 | 1383.41 | 985.74 | 538.77 | 604.61 | 4570 | 2562 | 644 | 828 |
| | 3 | 1474.76 | 1569.19 | 483.59 | 400.15 | 3683 | 5895 | 1218 | 952 |
| | 4 | 1282.29 | 903.13 | 502.99 | 335.69 | 2899 | 2471 | 640 | 442 |
| | 5 | 1240.13 | 811.17 | 317.38 | 407.5 | 4375 | 2154 | 299 | 572 |
| | 6 | 1681.18 | 1041.25 | 580.17 | 368.52 | 2335 | 2250 | 707 | 564 |
| | 7 | 2203.59 | 1430.54 | 446.23 | 541.81 | 3142 | 2324 | 643 | 821 |
| | 8 | 1472.71 | 1122.58 | 559.77 | 677.3 | 3442 | 3832 | 763 | 1044 |
| | 9 | 1518.68 | 1440.45 | 703.16 | 741.07 | 2715 | 4614 | 2120 | 1363 |
| | 10 | 1604.68 | 1577.81 | 516.85 | 507.5 | 5659 | 5547 | 1000 | 1139 |
| Two-day | 1 | 1114.08 | 945.24 | 999.92 | 797.65 | 1184 | 1197 | 377 | 316 |
| | 2 | *** | 884.34 | 489.7 | 666.86 | 1206 | 1248 | 0 | 0 |
| | 3 | *** | *** | 833.12 | 828.68 | 1213 | 1190 | 174 | 126 |
| | 4 | 2512.31 | 3411.7 | 1820.3 | 798.59 | 1251 | 1233 | 1134 | 204 |
| | 5 | *** | 3231.19 | 702.01 | 834.63 | 1157 | 1486 | 0 | 152 |
| | 6 | *** | 760.43 | 604.99 | 546.57 | 1207 | 834 | 0 | 0 |
| | 7 | 951.65 | 3240.92 | 661.56 | 583.51 | 1214 | 2431 | 0 | 0 |
| | 8 | 3485.08 | 1091.31 | 1056.46 | 751.69 | 1212 | 1275 | 248 | 130 |
| | 9 | *** | *** | 941.09 | 803.88 | 1144 | 1177 | 221 | 4 |
| | 10 | *** | *** | 807.13 | 857.56 | 1148 | 1241 | 187 | 174 |

the total costs including the start-up/shut-down, and generation costs for both traditional thermal and combined-cycle units. Physical constraints for combined-cycle units, as described in Sections III and IV, are captured. The detailed traditional thermal unit formulation is provided in [12]. In this system, there are 54 traditional thermal units and 12 combined-cycle units. As a comparison, we also test three other formulations: 1) "EBF", the edge-based formulation (EBF) proposed in [12]; 2) "TEBF", the edge-based formulation with min-up/-down constraints (9) and (10) replaced by tighter min-up/-down constraints (24) and (39); 3) "REBF", the edge-based formulation with the ramping constraints (17) and (18) replaced by tighter ramping constraints (40) - (50). All instances are solved by CPLEX 12.5 at Intel(R) Core(TM) i7-4500U 1.8GHz with 8G memory.

We study two groups of unit commitment problems: one-day and two-day unit commitment problems, respectively. For the one-day unit commitment problem, we use the default setting in CPLEX. For the two-day unit commitment problem, we set the optimality gap to be 0.05% and the time limit to be 3,600 seconds per run. For each problem, we generate ten different load profiles based on the forecast load following the method described in [12].

In Table X, we report the root-node information to show the effectiveness of our proposed strengthened formulation in tightening the LP relaxation gap. We first report the final MIP objective values and the root-node LP relaxation objective values for these four models (EBF, TEBF, REBF, and SEBF) at the root-node. For the same objective function of minimizing the total operating cost, the tighter the formulation is, the larger the LP relaxation objective value is. Then, we measure the tightness of the formulation by calculating the integrality gap,

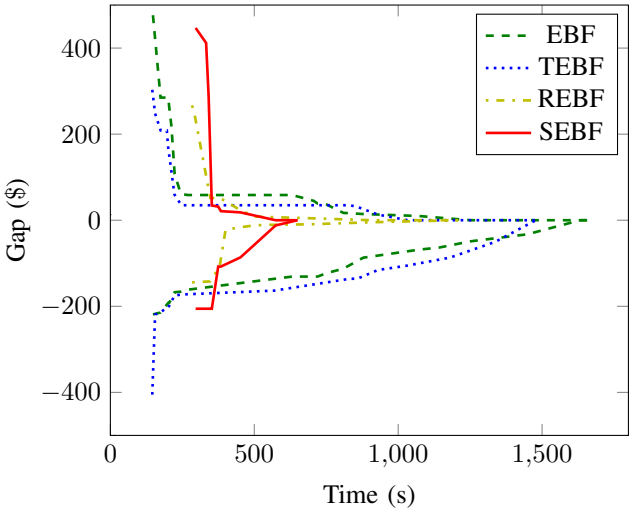


Fig. 5. Convergence evolution of Case 1 in One-Day UC

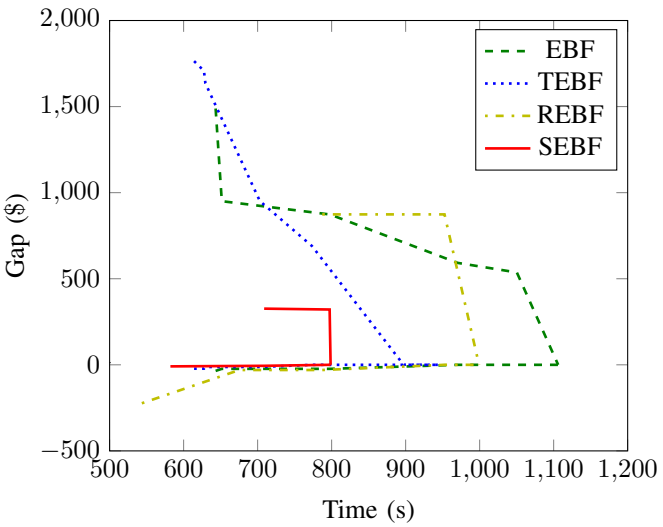


Fig. 6. Convergence evolution of Case 1 in Two-Day UC

which is defined as

$$\text{INTGap} = \frac{C_{MIP} - C_{LP}}{C_{MIP}},$$

where $C_{MIP}$ represents the objective value corresponding to the best integer solution obtained from these four models (EBF, TEBF, REBF, and SEBF), and $C_{LP}$ represents the LP relaxation objective value at the root node. Currently, most commercial MILP solvers solve the LP relaxation problems when they implement the branch-and-bound method. A small integrality gap can help reduce the searching time from the LP relaxation solution to the optimal integer solution and thus reduce the total computational time. From Table X, we can observe that for each instance the SEBF model provides a better lower bound (i.e., a larger LP relaxation objective value) than that provided by the EBF model. This results in a reduced integrality gap for the SEBF model.

In Table XI, we report the computational performances for all these models. We first report the computational time required to solve each instance. If CPLEX cannot solve the instance to optimality within the time limit, we use "***" to represent the corresponding computational time. We then report the number of branch-and-bound nodes explored. From Table XI, we can observe that our proposed tighter constraints and strong valid inequalities help reduce the computational time significantly. Meanwhile, the SEBF model leads to a much smaller number of branch-and-bound nodes than the EBF model does for most instances.

In Table XI, we can observe that solving the problem becomes more difficult as the size of the instance increases. In some instances (e.g., Cases 2, 3, 5, 6, 9, and 10 in two-day unit commitment), the EBF model cannot solve the problem to optimality within the time limit. In contrast, the SEBF model can solve all the instances under the same setting. Notice that it is unnecessary to branch in Cases 2, 6, and 7 for the SEBF model because CPLEX uses heuristic strategies and the cutting plane approach to find an optimal solution due to the small integrality gap and better LP relaxation lower bound.

In addition, we report the convergence process in Figs. 5 and 6. In these figures, the solid (resp. dashed, dotted, and dashdotted) line represents the convergence of the upper bound gap (denoted as "UBG") and lower bound gap (denoted as "LBG") of the SEBF (resp. EBF, TEBF, and REBF) model. The upper bound gap represents the difference between the upper bound (denoted as "UB") of MIP model at each iteration and the optimal objective value (denoted as "OBJ") of the MIP model. Correspondingly, the lower bound gap represents the difference between the lower bound (denoted as "LB") of the MIP model at each iteration and the optimal objective value (denoted as "OBJ") of the MIP model. In summary, we have the following relationships:

$$\Delta\text{UBG} = \text{UB} - \text{OBJ},$$
$$\Delta\text{LBG} = \text{LB} - \text{OBJ}.$$

From Figs. 5 and 6, we can observe that the SEBF model converges faster than the EBF model does. Meanwhile, we can observe that the SEBF model provides not only a better lower bound but also a better upper bound, since the proposed tighter constraints and strong valid inequalities help find better feasible integer solutions during the solution process.

## VI. Conclusions

In this paper, we focused on improving the computational performance to solve the unit commitment problems with combined-cycle units. We derived tighter min-up/-down time and ramping rate constraints. These constraints are tighter than the ones in the original formulation. Furthermore, we developed several families of strong valid inequalities focusing on strengthening ramping rate requirements to further reduce the searching space. Finally, the case studies demonstrated the effectiveness of our proposed strengthened edge-based formulation in reducing the computational time when solving the corresponding problems.

## REFERENCES


[1] "Generation Portfolio Analysis (MISO)." [Online]. Available: http://www.misomtep.org/generation-portfolio-analysis/.

[2] M. Tamayo, X. Yu, X. Wang, and J. Zhang, "Configuration based combined cycle model in market resource commitment," in *Proc. of 2013 IEEE Power and Energy Society General Meeting*, pp. 1–5.

[3] B. Blevins, "Combined-cycle unit modeling in the nodal design," *ERCOT, Taylor, Texas*, 2007. [Online]. Available: http://nodal.ercot.com/docs/pd/ida/wp/cc/IDA003_Combined_Cycle_Whitepaper_v_09.doc.

[4] S. Ammari and K. Cheung, "Advanced combined-cycle modeling," in *PowerTech (POWERTECH), 2013 IEEE Grenoble*, pp. 1–5.

[5] B. Lu and M. Shahidehpour, "Short-term scheduling of combined cycle units," *IEEE Trans. Power Syst.*, vol. 19, no. 3, pp. 1616–1625, 2004.

[6] T. Li and M. Shahidehpour, "Price-based unit commitment: a case of lagrangian relaxation versus mixed integer programming," *IEEE Trans. Power Syst.*, vol. 20, no. 4, pp. 2015–2025, 2005.

[7] A. Papavasiliou, Y. He, and A. Svoboda, "Self-commitment of combined cycle units under electricity price uncertainty," *IEEE Trans. Power Syst.*, vol. 30, no. 4, pp. 1690–1701, 2015.

[8] H. Hui, C.-N. Yu, F. Gao, and R. Surendran, "Combined cycle resource scheduling in ERCOT nodal market," in *Proc. of 2011 IEEE Power and Energy Society General Meeting*, pp. 1–8.

[9] Y. Chen, X. Wang, and Q. Wang, "Overcoming computational challenges on large scale security constrained unit commitment (SCUC) problems," *FERC*, 2014. [Online]. Available: http://www.ferc.gov/CalendarFiles/20140623080505-M1%20-%201%20-%20FERC2014_Chen_M1_06172014.pdf

[10] G. Morales-España, C. M. Correa-Posada, and A. Ramos, "Tight and compact MIP formulation of configuration-based combined-cycle units," *IEEE Trans. Power Syst.*, vol. 31, no. 2, pp. 1350–1359, 2016.

[11] C. Liu, M. Shahidehpour, Z. Li, and M. Fotuhi-Firuzabad, "Component and mode models for the short-term scheduling of combined-cycle units," *IEEE Trans. Power Syst.*, vol. 24, no. 2, pp. 976–990, 2009.

[12] L. Fan and Y. Guan, "An edge-based formulation for combined-cycle units," *IEEE Trans. Power Syst.*, vol. 31, no. 3, pp. 1809–1819, 2016.

[13] R. Jabr, "Tight polyhedral approximation for mixed-integer linear programming unit commitment formulations," *IET Gener. Transm. & Distrib.*, vol. 6, no. 11, pp. 1104–1111, 2012.

[14] E. Rothberg, "The CPLEX library: Presolve and cutting planes," in *4th Max-Planck Advanced Course on the Foundations of Computer Science (ADFOCS) 2003*, pp. 1–5.

[15] J. M. Arroyo and A. J. Conejo, "Optimal response of a thermal unit to an electricity spot market," *IEEE Trans. Power Syst.*, vol. 15, no. 3, pp. 1098–1104, 2000.

[16] D. Rajan and S. Takriti, "Minimum up/down polytopes of the unit commitment problem with start-up costs," *IBM Res. Rep.*, 2005.

[17] M. Carrión and J. M. Arroyo, "A computationally efficient mixed-integer linear formulation for the thermal unit commitment problem," *IEEE Trans. Power Syst.*, vol. 21, no. 3, pp. 1371–1378, 2006.

[18] A. Frangioni, C. Gentile, and F. Lacalandra, "Tighter approximated MILP formulations for unit commitment problems," *IEEE Trans. Power Syst.*, vol. 24, no. 1, pp. 105–113, 2009.

[19] J. Ostrowski, M. F. Anjos, and A. Vannelli, "Tight mixed integer linear programming formulations for the unit commitment problem," *IEEE Trans., Power Syst.*, vol. 27, no. 1, pp. 39–46, 2012.

[20] G. Morales-España, J. M. Latorre, and A. Ramos, "Tight and compact MILP formulation for the thermal unit commitment problem," *IEEE Trans. Power Syst.*, vol. 28, no. 4, pp. 4897–4908, 2013.

[21] L. A. Wolsey and G. L. Nemhauser, *Integer and Combinatorial Optimization*. John Wiley & Sons, 2014.

[22] "IEEE 118-bus system." [Online]. Available: https://sites.google.com/site/leifanee/dataset/.